Paper3: Metasomatic evolution of the Froland amphibolites during cooling and uplift – textural observations and geochemical evolution of hydrous minerals

Bjørn Eske Sørensen
Department of Geology and Mineral Resources Engineering, Norwegian University of Science and Technology (NTNU), N7491 Trondheim, Norway
(bjorn.sørensen@ntnu.no)

Rune Berg Larsen
Department of Geology and Mineral Resources Engineering, Norwegian University of Science and Technology (NTNU), N7491 Trondheim, Norway
(rune.larsen@ntnu.no)

Håkon Austrheim
Department of Earth Sciences, University of Oslo, N-0316 Oslo, Norway
(h.o.austrheim@geo.uio.no)

Abstract

This study addresses the metasomatic alteration of ortho amphibolites, in the Froland segment of the Bamble sector, South Norway. High salinity brines with near constant salinities of c. 30 wt% solvents infiltrated and metasomatised the amphibolites throughout cooling and uplift. Potassic alteration and biotite formation comprise the earliest deductible alteration event and is seen as overgrowth on amphiboles. Alteration begins by ferro tschermakite formation that gradually becomes richer in Mg and depleted in Fe, K, Na, Al and Cl and, finally, terminates with Cl poor actinolite (XMg ≈ 0.9). Simultaneously, biotite experiences metasomatic alteration that is strongly correlated with the coexisting calcic amphibole.

The compositional changes reflect the complex interaction between brine fluids and hydrous minerals during cooling and uplift. Accordingly, the brine fluids fully control the composition of Fe-Mg silicates. Therefore, the models arguing that the Cl content of biotite is a function of the original Fe/Mg ratio of the mineral, fluid composition and PT-conditions (Munoz, 1992; Munoz and Swenson, 1981) can not explain the Froland amphiboles and biotites. Rather we find that the composition of the halogen bearing Fe-Mg silicates is partially controlled by the aqueous fluid composition along with P and T. Two models may explain the biotite and amphibole chemical zonation.

Model 1: zoning reflects interactions with a fluid of varying composition at fixed P and T. This model explains the compositional zoning observed by Kullerud and co-workers (1995; 1996; 1999), but cannot fully explain the compositional zoning observed in our study because the fluid salinity is constant.

Model 2: compositional zoning reflects interaction with a fluid having constant halogen contents during gradually changing PT-conditions. Model 2 is preferred in the current study because biotites and amphiboles in our study formed during cooling and exhumation with constant salinities of the coexisting fluid.

In intensively altered areas the original amphibolite mineralogy is entirely replaced. Here, we observe the largescale metasomatic processes in a small scale version. For example following this pattern: Amphibolite with small amount of biotite (host rock)→ Zone1: biotite-plagioclase zone → Zone2: amphibole-plagioclase zone → Zone3: Plagioclase + calcite + apatite zone → Zone3a: pyrrhotite + ilmenite (rutile +titanite) ± amphibole + calcite+ chalcopyrite + apatite in the core of the plagioclase rich Zone3. Accordingly, ore forming elements such as Cu, Mo, Au and Fe are mobilised from the deeper part of the alteration zone to shallower levels of the shearzone complex (see also Cameron et al., 1993)

1 Outline and summary

The Bamble sector is renowned for its fluid-related metasomatic rocks. However, systematic studies of the retrograde evolution of the volatile fluids are rare and fragmentary.

The aim of this study is to understand the parameters that control the metasomatic processes in the Froland area of the Bamble Sector. The chemical evolution of halogen bearing minerals including amphiboles, biotites, apatite and scapolite are studied in extension of the fluid inclusion studies reported elsewhere (Paper 2, Sørensen and Larsen). Amphiboles are imperative in understanding the retrograde evolution given that they are present from upper amphibolite facies peak PT-conditions to lower green schist facies. The results reported here agree with the PT-X_{fluid} path deduced by Sørensen and Larsen (2007b, paper 2). Contrary to earlier studies, the metasomatic evolution reported here is dominated by potassic alteration.

In the Froland area fluid inclusion studies document that brine fluids of near constant salinities dominated throughout cooling and exhumation (Sørensen and Larsen, 2007b, paper 2). Accordingly, we argue that the univariant trends of amphibole and biotite reflects the interaction with an externally derived fluid with near constant salinity during falling P-T conditions.

Geochemical trends are combined with textural studies to establish a chronological scenario. Timing of alteration in the Froland area partially differs from previous studies elsewhere in the Bamble Sector. For example, contrary to other studies, the early stages of potassic alteration precede the sodic-calcic alteration reported from the eastern Bamble (e.g. Brøgger, 1934) (see background). We also suggest that most alteration occurred at constant Cl/H_2O ratio. The thermodynamic implications of

constant Cl/H_2O ratios is that modelling of the metasomatic processes in the Bamble Sector, is the results of fluid rock interaction with a fluid of constant salinity during variable P and T. Therefore, the high salinity of the fluids controls metasomatic processes and ore formation in the Bamble Sector.

Ultimately, this study support that the Mg-Cl avoidance models stating that energetic interaction between octahedral cations Mg and Fe originally present in the mineral is the dominant control of the $Cl \leftrightarrow OH$ exchange for amphibole and biotite is not applicable and may actually be void as it was also suggested by Kullerud (2000).

In future thermodynamic modelling, we suggest that coexisting biotite and amphibole is used in order to avoid the effects caused by the bulk rock Fe/Mg ratio. A full Thermodynamic model should include not only the chemical potentials of Fe, Mg, Cl and OH species in the solids but also aqueous species because of Fe and Mg exchange between biotite/amphibole and a fluid phase. The presence of other complexing ions in the fluid such S-species may also play an important role in the exchange of metal ions between silicates and a fluid. Until better calibrations are available Cl in amphibole or biotite cannot be used as a quantitative assessment of fluid composition. Fluid inclusions are the most reliable source on the composition of paleo fluids.

2 Fluid alteration in the Bamble Sector

Metasomatic processes are common in Bamble and encompasses scapolitisation, albitisation, abundant apatite and more rare dolomite veining (Dahlgren et al., 1993). Amphibole-scapolite rocks are known from several localities (Korneliussen et al., 2000) and they are commonly associated with enstatite phlogopite rocks and albitites of controversial origin. Metasomatism is restricted to diffuse, but mapable associated with faults, joints and lithological contacts between metagabbros and metasedimentary units (Nijland and Touret, 2001). Alteration zones comprise a network that may be characterised as a regional plumbing network (Nijland and Touret, 2001). Commonly, fluid alteration facilitates large scale mass transfer. This is supported by the spatial relation between ore deposits and zones of massive alteration. Sodic alteration is most conspicuous in comprising long known albitites - scapolite - hornblende rocks (Brøgger, 1934; Bugge, 1965; Elliott, 1966; Jøsang, 1966; Munz et al., 1994; Munz et al., 1995). Structurally controlled apatite bearing Fe/Cu sulfide/oxide deposits and rutile deposits structurally related to the scapotilization zones (Korneliussen et al., 2000). (Brøgger, 1934) suggested that the breccia-related iron ores at Langøy were products of leaching processes involving metagabbros and (Korneliussen et al., 2000) suggest that similar models may as well account for other ore deposits.

Nijland et al.(1993a) studied the geochemistry of hydrous minerals in amphibolites from localities in the Bamble sector in an approach to understand the fluid composition in the Bamble sector during prograde as well as retrograde PT-t paths. They conclude that systematic variations of the fluid composition from granulite to amphibolite facies

areas are absent. Compositional variations are encountered on a much more localised scale (e.g. Nijland et al., 1993a).

Scapolite commonly occur as replacement of plagioclase along grain boundaries, indicating that it is a late phase (Nijland et al., 1993a) in the Froland area, whereas it seem to be an earlier phase in more intensely scapolitised rocks in the eastern part of the Bamble sector. The formation of scapolite in the Froland area relates to introduction of saline aqueous fluids during retrogression (Sørensen and Larsen, 2007b, paper 2).

More intense scapolitisation is observed at Ødegårdens Verk where scapolitisation of metagabbro formed a rock composed of scapolite-phlogopite-rutile rocks intersected ny phlogopite-enstatite-apatite veins and albitites (Elliott, 1966). Scapolite in the hornblende scapolite rock is a chlorine rich marialite with the A site fully occupied by Cl and 3.7 atoms Al p.f.u., rather than the 3.0 allocation suggested by plagioclase substitution (Lieftink et al., 1993). The hornblendes at Ødegårdens Verk also display rimward zoning from Cl and alkali rich cores to Al and Cl poor rims that also are enriched in (what?) (Lieftink et al., 1994). Veins comprising Cl-apatite, enstatite and phlogopite are also common at Ødegårdens Verk. They are older than the scapolite-hornblende rock and were partially replaced by hydroxyl-flour apatite and hornblende during later scapolitisation (Lieftink et al., 1994). The Cl-apatite carry trails and patches of monazite and xenotime in areas altered to a hydroxyl-flour apatite that formed during amphibolite facies alteration (Lieftink et al., 1994). This interpretation was matched by experiments with fluids of variable composition on Cl-apatite from Ødegårdens Verk by Harlov et al. (2002) who argue that fluid composition is more important than P. The hydroxyl-flour apatite with trails and patches was reproduced by H_2O and F bearing fluid.

Albititites are also a common result of sodic alteration in the Bamble Sector, and comprise a wide range of expressions (Nijland and Touret, 2001). Albitisation was later than the scapolitisation given that scapolite is replaced by albite (Brøgger, 1934).

On the contrary, potassic alteration are not previously reported from the Bamble sector, although biotite is common in the more altered parts of the metagabbro at Langøy, eastern Bamble (Austrheim, 2006 pers. comm.) and Cameron (1993b) reported reintroduction of LILE including K and chalcophile elements that were leached during granulite and amphibolite facies metamorphism, during retrogression on Tromøy. In the studied area potassic alteration is much more pronounced than sodic alteration types. The most common expression of potassic alteration is the introduction of biotite into the amphibolites., However, potassic alteration also include grey K-feldspar together with actinolite-titanite rocks in the most intensively altered parts. Because these rocks were not described before in the Bamble we will discuss their petrography and outcrop textures in detail in section 4.1.

The alteration processes is strongly influenced by fluid composition, P and T. In the only systematic study of the retrograde fluid evolution (paper 2, Sørensen and Larsen, 2007b) it is documented that the fluid composition in the Froland area comprise brines

with 30 wt% salts throughout cooling and uplift of the area. Three crucial fluid evolutionary stages could be unravelled:

FIA2. Early retrograde fluids in vein quartz comprising low salinity CO_2-rich fluids and H_2O rich eutectic salinity NaCl-KCl-H_2O-CO_2 brines associated with biotite-amphibole assemblages bordering en echelon quartz veins in amphibolite.

FIA3. H_2O-NaCl-$CaCl_2$ brines with 25 wt% NaCl and 6 wt% $CaCl_2$. involved in localised scapolitisation and replacement of rutile by titanite in silisic gneisses and replacement of ilmenite by titanite in amphibolites.

FIA4: $CaCl_2$ rich aqueous fluids in late vug assemblages comprising tremolite, epidote, calcite, pyrite and apophyllite. Inclusions are found in calcite and in cores of epidote grains. FIA4 was modelled in the binary $CaCl_2$-H_2O system. Variations in final melting of antarcticite suggest a decreasing $CaCl_2$ salinity over time from 36 wt% in early inclusions to 31 wt% in late inclusions. Late inclusions relates to increased Fe-content in epidote and it is suggested that the Fe^{3+} content increased over time in agreement with the lowering of the eutectic melting temperature from the ideal of -52°C in the binary $CaCl_2$-H_2O system.

Sørensen (2007b, paper 2) used observations of fluid inclusions and calcsilicate assemblages in combination with a re-interpretation of the mineral paragenetic data presented by Nijland et al. (1993b) to re-evaluate the cooling and exhumation path of the Bamble Sector (Figure 1). The retrograde fluids may partially be superimposed upon the PT-evolution of the Froland area (Figure 1). More details in (Sørensen and Larsen, 2007b, paper 2). In summary, the cooling and uplift path begins by the simultaneous formation of tremolite + sanidine and tremolite + sanidine + calcite assemblages at c. 626-636°C and 7 kb. The next stage agree with MII (ky + chl + ms) and MIII (ma +crn) of (Nijland et al., 1993b). The pressure is uncertain although a path may be extended from this stage to the isochore of FIA3. Because the fluid inclusions in FIA3 are well preserved showing no evidence of post entrapment modification the exhumation path could not have deviated more than 2 kb from the FIA3 isochore. The last part of the cooling and exhumation path is constrained by MV at 2-3 kb and 175-280°C (Nijland et al., 1993b; Touret, 1985) The PT-path preserves the main characteristics of the path published by Nijland et al.(1993b), but the uplift is shifted 100°C toward lower temperatures and is in better agreement with the dominance of cataclastic microstructures in thrust related structures. A shift between potassic and sodic-calcic alteration occurred between FIA2 and FIA3. The Shift between MII and MIII probably correlate with the shift in alteration types (Figure 1).

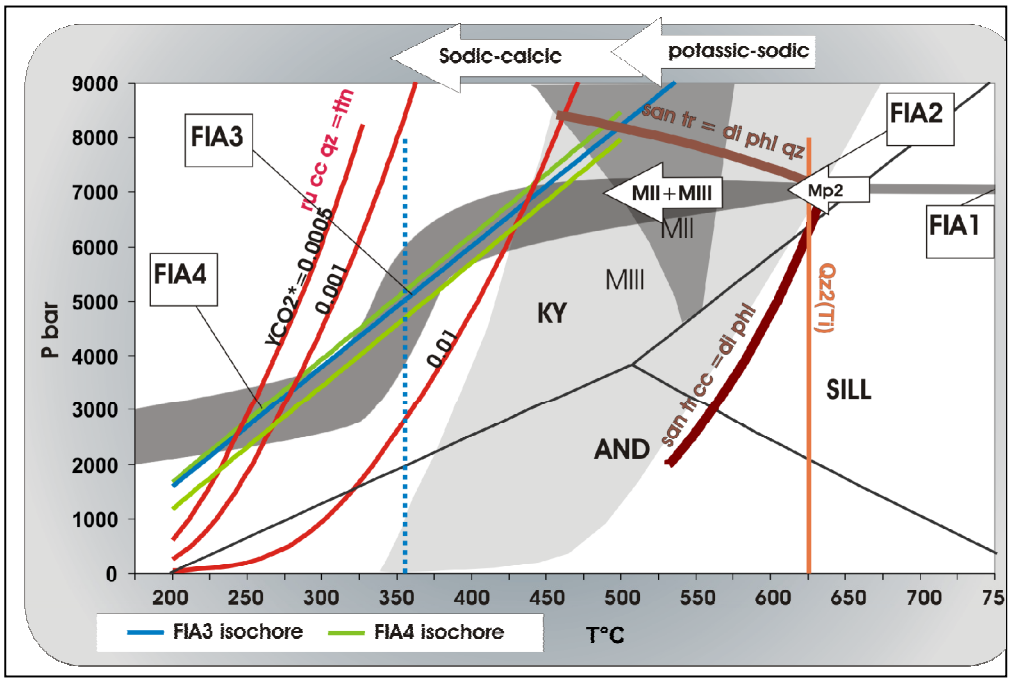

Figure 1: Tentative PT-Xfluid path of the study area, with possible implication for to uplift path of the Bamble sector. The PT-Xfluid path is assembled using a combination of mineral paragenetic and fluid inclusions data. Because fluid inclusions and mineral parageneses that are simple enough to be portrayed quantitatively in PT-space are not always present the correctness of the PT-path rely on textural correlations between assemblages in one rock type and fluid inclusions found in other rock types. Arrows on the top of the diagram indicate condition when alteration changed from potassic-sodic to sodic calcic. From Sørensen (2007b, paper 2). For a more detailed discussion of the derivation of the PT-path see Sørensen (2007b, paper 2). Reactions are written such that the high temperature assemblage is to the right of the = sign.

3 Geological setting

The rocks included in this study comprise quartzites, amphibolites and calc-silicate lithologies from the Froland area, Bamble sector, South Norway (Figure 2). The Bamble sector is part of the South West Scandinavian domain (SSD) that is divided into a number of segments bounded by regional shear zones and thrusts that formed during the Sveconorwegian orogeny (Ahall and Gower, 1997; Bingen et al., 2002). The Bamble sector is interpreted as the mid-crustal part of a volcanic arc complex (Knudsen and Andersen, 1999). The Bamble sector was accreted to the Telemark terrain during an early Sveconorwegian (1,15-1,10 Ga) event (Bingen et al., 2002; 2001).

Structurally, the Bamble sector comprises a SW to NE linear deformation belt with onshore dimensions of 20-40 km times 140-150 km (Figure 2).

Supracrustal lithologies of amphibolite to granulite facies metasedimentary and metavolcanic rocks dominate the belt and is intruded by numerous mafic stocks and dykes as well as granitiod plutons and pegmatites (Starmer, 1991; Starmer, 1993; Starmer, 1996). The Supracrustal suite was deposited in two inter-orogenic periods of the Gothian orogeny at 1,85-1,7 Ga (Knudsen et al., 1997) and 1,5-1,2 Ga (Bingen et al., 1998) respectively. Recent studies confirmed Sveconorwegian high-grade metamorphic overprinting throughout the Bamble sector (Bingen et al., 1998; Bingen and Van-Breemen, 1998; Cosca et al., 1998; Johansson and Kullerud, 1993; Knudsen, 1996; Kullerud and Machado, 1991; Kullerud and Dahlgren, 1993).

Generally, the foliation trends NE-SW in the Bamble belt (Falkum and Petersen, 1980). Based on structural trends, the Bamble sector is divided in two domains (Falkum and Petersen, 1980):

-*The eastern sub-region* (main zone) in the coastal area is dominated by intense shear folding with a NE-orientation, most other directions being rotated into parallelism by a dextral strike slip regime. The structural pattern is dominated by tight isoclinal folds and well developed mineral lineations. Older structures are preserved in rigid bodies.

- *The Northern border* constituting a transitional zone 10-15 km wide, is characterized by moderate shear folding where NE-SW trending structures of the Bamble sector are superimposed on former NW-SE trending folds of the Setesdal gneisses. The transition zone commonly shows interference between the two structural events.

The Bamble sector features well preserved granulite facies rocks and distinctive metamorphic zones gradually going from amphibolite facies in north to granulite facies along the coast. Peak metamorphic conditions are well constrained, both in terms of P, T and fluid evolution.

Traditionally the Bamble sector is divided into four coast parallel regions labelled A-D (Field et al., 1980; Lamb et al., 1986; Smalley et al., 1983):

A: Amphibolite facies, as defined by absence of metamorphic orthopyroxene in metabasite.

B: Granulite facies; primarily comprising acid to intermediate host gneisses with a broadly granitic mineralogy, separated from A by an orthopyroxene isograde in metabasites.

C: First occurrence of charnokitic gneiss (K-feldspar, plagioclase, orthopyroxene and quartz).

D: Region within the granulite facies area with low concentrations of potassium and low concentration of LILE, REE and chalcophile elements, especially Au, Sb, As and S.

Earlier studies of the Bamble sector placed the area of highest temperature in the coastal region near Arendal and Tromøy in region D which was thought to be LILE depleted during peak metamorphism. However recent studies imply that low LILE concentration reflects the origin of the mafic gneisses rather than granulite facies depletion (Knudsen and Andersen, 1999). Furthermore, geothermobarometry show that

the temperature in zones C and D are comparable (Harlov, 1992; Harlov, 2000a; Knudsen and Lidwin, 1996; Nijland and Maijer, 1993). Accordingly, zone D is not a separate metamorphic zone (Harlov, 2000b). Geothermobarometry of mineral equilibria imply that the highest temperatures probably were situated inland in a NW-SE oriented thermal dome with peak T at 830°C in the granulite facies area (Zones B and C) and peak T=750-700°C in the so called amphibolite facies area (zone A) (Nijland and Maijer, 1993). I.e. the entire region was actually exposed to granulite facies metamorphism.

Metamorphic fluids developed from pure CO_2 +N_2 ±CH_4 inclusions in the granulite facies to mixed H_2O-CO_2 fluids in the amphibolite facies (Touret, 1971; Touret, 1972; Touret, 1985). Some authors suggest a magmatic origin of the CO_2 rich fluids (Knudsen and Lidwin, 1996; Van den Kerkhof et al., 1994). The presence of CO_2 rich fluids during peak granulite facies metamorphism is confirmed by titaniferrous magnetite-ilmenite thermometry and tintaniferous magnetite –ilmenite-orthopyroxene-quartz oxygen barometry, implying that the stable COH-fluid phase at $LOGfO_2$ = -11 to -14 estimated for the peak PT-conditions (800°C and 7.5 kbar) is CO_2 for both region C and D (Harlov, 2000b).

Given that the structures of the Setesdal district are rotated into the foliations of the Bamble belt, it is inferred that the structures in the Bamble belt comprise the youngest structural event in the evolution of the South Norwegian basement. Following the strike-slip deformation, the Bamble sector was thrust on top of the Setesdal sector. In many places, the main thrust zone follows the Porsgrund Kristiansand fault, but thrusts are also identified to the east of the fault (e.g Touret, 1968). Thrusting probably began in epidote-amphibolite facies and progressed through lower greenshist facies as exhumation proceeded (e.g Touret, 1968). Finally extensional tectonics depressed the SE Bamble block. Evidence of thrusting is indisputable, although the kinematic evolution during thrusting is poorly understood and mostly inferred from, mapping and large scale observation by Starmer (1987; 1991; 1993; 1996) and (e.g. Henderson and Ihlen, 2004).

Thrust related greenshist facies deformation generated quartz mylonites (Morton et al., 1970), mainly comprising quartz and muscovite (Morton et al., 1970). Grain size reduction in the mylonites is considerable i.e. from cm-size to microns-size. Thrust related deformation terminated with brittle deformation, cataclasites and brecciation as exhumation proceeded and the temperatures lowered (e.g Touret, 1968).

Recently, Henderson & Ihlen (2004) documented ductile deformation of synkinematic pegmatites. They infer that thrust related deformation in the Bamble sector was incremental with long periods of ductile deformation interrupted by short periods of high strain rate leading to fracturing and injection of the syntectonic pegmatites.

Using the retrograde P-T path of Nijland et al. (1993b) the uplift and cooling rates were constrained to ~3°-8°C/Ma at 725-550°C, and cooling rates of ~2°-4°C/Ma in the interval 550-300°C (Cosca et al., 1998). Initial cooling of the Bamble sector approached isobaric conditions (dP/dT=2bars/°C) from 725-550°C, but was followed

by near isothermal uplift (dP/dT=30bars/°C) in the temperature interval 550-300°C (Cosca et al., 1998). Following the relatively fast exhumation path, the Bamble sector experienced near isobaric cooling from 300°C and onwards (Cosca et al., 1998). The very low temperature (<300°C) path is constrained by late prehnite and pumpelyite together with fluid inclusion data (Touret and Olsen, 1985).

Amphibolites are common in the Bamble sector. They feature four expressions (Nijland et al., 1993a):

1. Concordant amphibolite bands intercalated with gneisses (Brøgger, 1934; Starmer, 1985).
2. Entirely metamorphosed but discordant plutons like the Vimme amphibolite (Nijland, 1989)
3. Partly amphibolitised "hyperites" with cores of coronitic gabro, which are increasingly amphibolitised towards their margins (Brickwood and Craig, 1987; Brøgger, 1934; Bugge, 1940).

Nijland (1995) studied the geochemistry of the amphibolites in the Bamble sector and documented that the majority are of an igneous origin. The amphibolites are commonly subjected to significant metasomatic processes affecting the mineralogy (Brøgger, 1934; Frodesen, 1968; Konnerup-Madsen, 1979).

4 Results

4.1 Field and petrographic observations

4.1.1 Introduction

Five main localities were used in this study, all situated within in a 5 square kilometre area (Figure 2).

Locality 1

Represents the best preserved high grade evolution and provides detailed information on the formation of garnet amphibolite from coronitic gabbro.

Locality 2 and 3

Features well preserved garnet amphibolite, but does not preserve any coronitic gabbro.

Locality 4

En echelon quartz veins in amphibolite bordered by potassic alteration of amphibolite. Veins vary in thickness from dm to m thickness. En echelon veins belonging to this type are common in the Froland area.

Locality 5

The most pronounced amphibolite alteration. A vertical section through a zone of intensive alteration of amphibolite is exposed at a quarry. The orientation of the hydrothermal alteration zone and the local foliation is almost perpendicular to the regional foliation trend, but parallel to the orientation of splay offs of thrust related

mylonites in the area (see map in Touret, 1968). The SE and NW facing walls are most informative, concerning the architecture of the alteration zone. Three rock types are recognized in the quarry; amphibolite and quartz-biotite-microcline-plagioclase-tourmaline gneiss. Furthest to the East is gneiss, followed by amphibolite and then more gneiss. Calcsilicate rock is sandwiched between gneiss and amphibolite. Details on the calcsilicates may be found elsewhere (Sørensen and Larsen, 2007b, paper 2).
East of the main alteration zone the gneiss is bleached and deformed to mylonitic gneiss with grey stripes marking the presence of graphite. Flakes of graphite define the foliation together with biotite and red-brown tourmaline. Quartz texture is typical of mylonitic gneiss with quartz grain boundaries showing evidence of high temperature grain boundary migration recrystallisation (GBM). Plagioclase and feldspar grains vary in shape from irregular to lens shaped. The lens shaped feldspar show variable degrees of asymmetry, with asymmetric feldspars defining a shear sense in agreement with an upward movement of the SW block. Partly bleached leucosomes of dravitic tourmaline and slightly bluish quartz are preserved as relics in the deformed and bleached gneiss. West of the alteration zone, the gneiss is darker and does not carry graphite. Bluish quartz in the quartz-dravite leucosomes gives a distinctive dark colour. Alteration occur as localised fracture related veins, related to introduction of aqueous brines (see Sørensen and Larsen, 2007b, paper 2). In spite of the different appearance of the two gneiss units we suggest that they were formed from the same protolith due to many similarities in the mineralogy. Because of the alteration pattern it is evident that main fluid alteration occurred in the hanging wall rocks, to the East.

Main types of calcic amphiboles

Six main types of amphibole were observed, hereafter denoted **Amp1, Amp1a, Amp2, Amp3, Amp3a** and **Amp4** Table 1). **Amp1, Amp1a and Amp2** comprises the likely high-grade amphiboles, whereas **Amp3 and Amp4** formed during exhumation. The distinction between amphibole types 3 and 4 is purely descriptive as they represent a continuous series from magnesio-hornblendes to actinolite**.**

Table 1: Amphibole types, description and mode of occurrence

	Type	Classification	Type of occurrence	locality
cores	Amp1	Ferri/ferro-tschermakite	Garnet amphibolite.	1, 2 and 3
	Amp1a	Hastingsite/Ferro-pargasite	Garnet-quartz symplectite	1, 2
	Amp2	Ferro-pargasite	Amphibolite, not garnet bearing.	5
rims	Amp3	Magnesio-hornblende	Overgrowth rims and in decussate textures together with biotite and plagioclase	5
	Amp3a	Ferropargasite/Ferrotscermakite	Overgrowth rims on amphiboles in association with biotite	1, 2 and 3
	Amp4	Actinolite-Magnesiohornblende to Actinolite	Same as Amp3	5

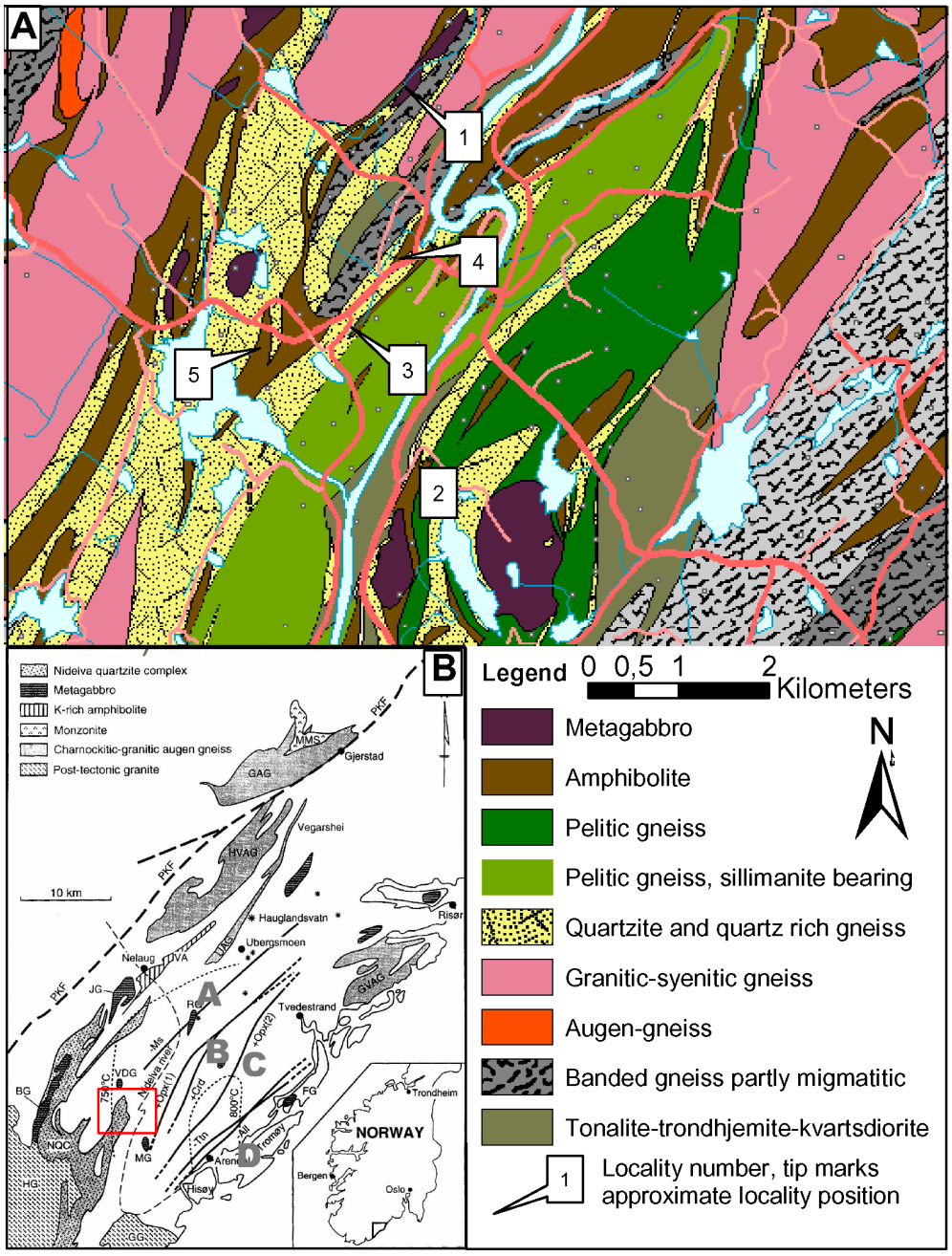

Figure 2: Geological maps. A) Detailed map of the investigated area. Modified from Geological Survey of Norway N-50 berggrunns kart 16123 Nelaug and 16114 Arendal. Geographic data (roads, lakes and rivers) are added for easy orientation (source:

www.geonorge.no). B) Overview map of the Bamble Sector displaying the most important rock units (see legend on map). Insert show the position of the Bamble Sector in South Norway. Red square denotes the position of the study area shown in A. From Nijland et al. (1998). Also shown in B are the metamorphic zones in the Bamble Sector.

4.1.2 Amphibolitisation during prograde metamorphism (type locality: locality 1)

The transition from a coronitic gabbro to garnet-amphibolite with cm-dm-sized garnet and black amphibole is observed macroscopically in the field (Figure 3). Field observations define the following units:

1. Coronitic gabbro
2. Garnet-amphibolite with small garnet and preservation of subophitic texture.
3. Banded garnet-amphibolite with cm-dm sized garnets, and banding between dark amphibole rich layers and light plagioclase rich layers. Garnets are in the dark layers and are surrounded by black amphibole rims.
4. Garnet-quartz and quartz-plagioclase symplectites.
5. Mixture of Gneiss/quartzite/amphibolite.
6. Extremely coarse-grained quartzite with blue quartz.
7. Pegmatites intersecting all the other units.
8.

The magmatic ophitic texture is well preserved with lath shaped plagioclase crystals surrounding grains of pyroxene (Figure 5). Plagioclase and pyroxene are never in contact but separated by rims of amphibole± garnet. The interiors of pyroxene grains are cut by numerous cracks with alteration to amphibole in a mesh texture.

The change from coronitic gabbro to the garnet amphibolite is gradual and can be followed on the map scale (Figure 3). Over half a meter, pyroxene grains in the gabbro are entirely altered to a garnet-amphibolite (1). Garnet-amphibolite (1) grades into garnet-amphibolite (2) over a distance of about two meters. Garnet-amphibolite (2) follows garnet-amphibolite (1) and is distributed as a 6 m thick layer. Garnets are always partially altered to chlorite along joints.

While fresh looking garnets are irregular in shape altered garnets are rounded (Figure 4c). This observation show that the garnets grew in a low strain environment and that deformation began after the growth of the garnets, resulting in partial breakdown. Towards the boundary to unit (5) the amount of garnet gradually decreases, but the black amphibole rich layers persists as dark schlieren. Unit (5) is a mixture of gneiss, amphibolite and quartzite. The widespread occurrence of green amphibole (field colour) in this unit indicates that it was subjected to more retrogression than the other units. Sigmoidal bodies featuring deformed quartz schlieren imply a dextral sense of shear during retrogression, as also suggested by NNE striking foliation being rotated into NE striking foliations (Figure 3).

In the completely amphibolitised area the garnet amphibolite consist of amphibole, plagioclase, garnet and minor ilmenite. The texture is granoblastic with interlocking amphibole and plagioclase surrounding large garnets (Figure 5). The Amphibole is brown tschermakite commonly displaying twins. Generally the amphiboles are homogeneous. However, they have overgrowth rims of more greenish blue amphibole, often associated with biotite (se next section). Amphibole commonly occur as inclusions in poikiloblastic garnets. Plagioclase contains both polysynthetic twinning and commonly also twins tapering towards pointed end that are interpreted as deformation twins cutting through the polysynthetic twinning (Figure 5).

The garnet-quartz and quartz-plagioclase symplectites are not evenly distributed in the amphibolite, but mostly occur in two areas (see Figure 3). When properly exposed, it appears they occur as lensoid bodies connected by dark amphibole rich bands intersecting the garnet amphibolite. The intergrowth texture between garnet and quartz suggest that they grew simultaneously. The texture and the distribution of symplectites in lenses and zones imply an igneous origin, perhaps as partial migmatitic melts.

The mineralogy of the garnet-quartz symplectitic intergrowth is amphibole, biotite, feldspar and garnet and an opaque assemblage of ilmenite, pyrrhotite, chalcopyrite and minor rutile on the edges of ilmenite grains. Amphiboles in the garnet-quartz symplectites are considerably darker than in the garnet amphibolite. As ilmenite occurs as inclusions within the garnet, it is interpreted as primary. Ilmenite also occurs as rounded blebs, perhaps an indication of possible melt immiscibility. Biotite, Epidote and pyrrhotite are secondary and relate to the formation of blue-green rims on the dark olive green amphibole cores (see next section).

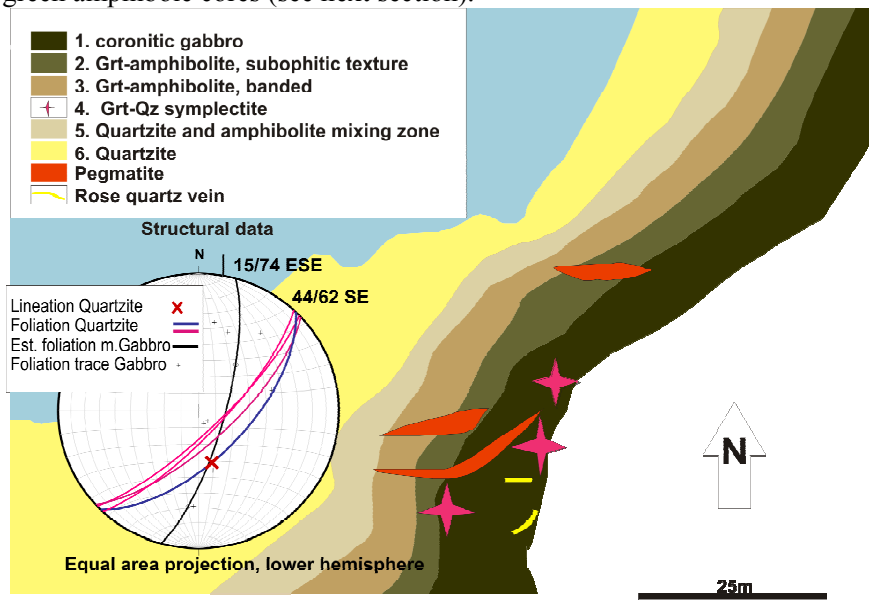

Figure 3: Detailed map of locality 1, showing the transition from gabbro to garnet amphibolite. Insert displays the structural observation from the locality, foliations are

stated as direction/dip. NNE striking foliations inferred to be early are partly rotated in NE striking structures during dextral shear strike-slip deformation. Lineation observed in quartzite reflects the intersection between the old and the new foliation. See text for discussion.

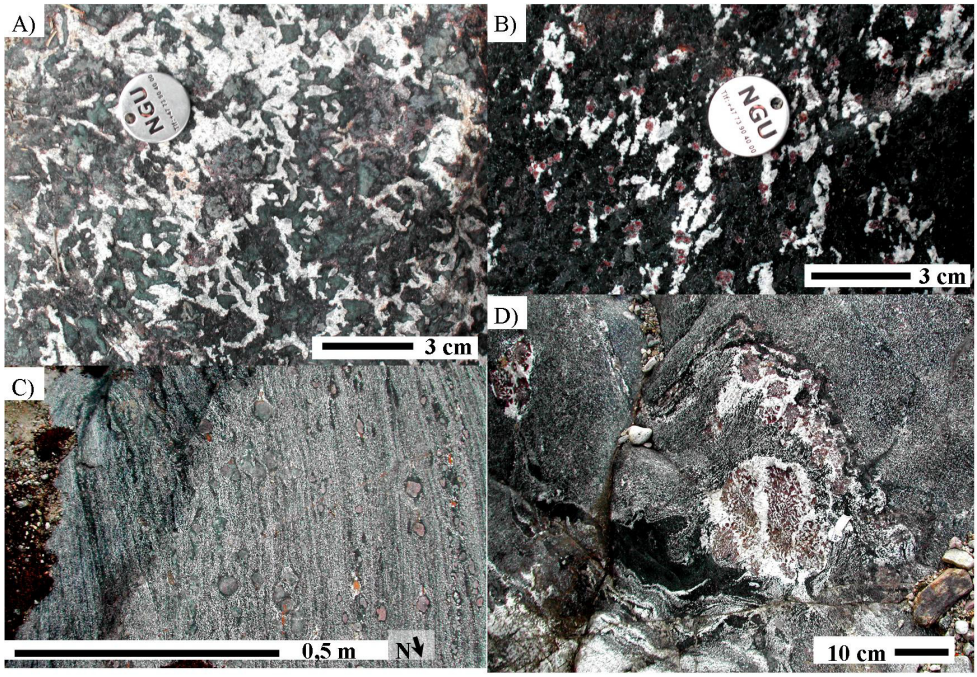

Figure 4: Field observations related to amphibolitisation of gabbro and garnet quartz symplectites. A) Coronitic gabbro with subophitic texture. B) Completely amphibolitised gabbro with preserved subophitic texture and a static appearance. C) Completely evolved deformed garnet amphibolite, subophitic texture not recognisable. D) Garnet quartz symplectite in garnet amphibolite.

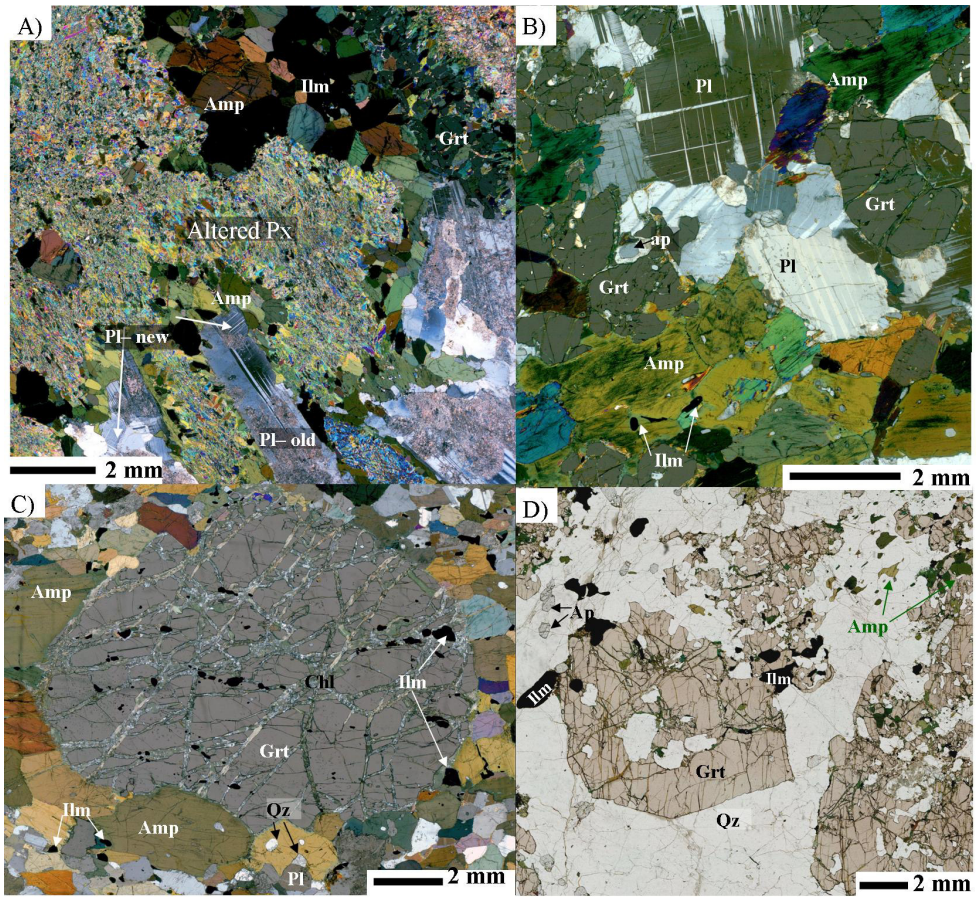

Figure 5: Petrographic observations related to the formation of garnet amphibolite and garnte quartz symplectites. A) Coronitic gabbro displaying relic pyroxene overgrown by hornblendeagianst plagioclase. Garnet is for between ilmenite and plagiaclase. B) Completely amphibolitised gabbro comprising plagioclase, amphibole, garnet and minor ilmenite. C) Granoblastic banded garnet amphibolite with cm-sized garnet in matrix of tschermakitic amphibole and plagioclase. Ilmenite present inside garnet as well as in the matrix

4.1.3 Retrograde alteration of amphibolite

Retrograde alteration patterns show considerable spatial variation. The most common alteration is potassic/sodic. Sodic/calcic alteration is later and more local. The alteration events comprise three main groups, i.e. potassic alteration with biotite, potassic alteration with k-feldspar and sodic calcic alteration with scapolitisation (Table 2).

Potassic alteration with biotite is the earliest observed alteration type (Alt1) and is divided into four main groups. Altered amphibole rims associated with biotite (Alt1a) is observed at all localities.

The cores of the amphiboles are commonly dark green, brownish green or brown in thin section. They are overgrown by distinctive amphibole rims (Figure 6). This is interpreted as reaction rims related to the formation of the biotite grains. The amphibole rims gradually change from dark blue-green (Amp3a) to green (Amp3) and almost colourless (Amp4) (Figure 6). This colour variation marks the transition from ferro-tschermakite through magnesiohornblende to actinolite with large compositional variations within a single locality and even a single sample (see section 4.2.1). In parallel with the amphibole evolution, biotite also change colour. Dark blue green overgrowths on amphibole (Amp3a) are common at localities 1, 2 and 3, whereas lighter coloured amphiboles (Amp3 and Amp4) are more common at localities 4 and 5. More extreme potassic alteration involving complete replacement of the original amphibolite mineralogy is also common (see next sections).

Decussate magnesiohornblende (Amp3) together with biotite, plagioclase, apatite Ilmenite, partly alter to titanite is commonly observed in reaction zones in amphibolite surrounding en echelon quartz veins (locality 4) (Figure 7). These reaction zones are associated with dm thick rims of black tourmaline bordering quartz veins and followed by bands of decussate amphibole-biotite (Figure 7b). Plagioclase is almost completely altered, whereas biotite and particularly amphibole is well preserved. Biotite is partially replaced by K-feldspar and ilmenite is partly replaced by titanite (Figure 7c). Small amounts of pyrrhotite occur in the alteration zones in the plagioclase and amphibole rich and biotite poor domains. Similar textures are also seen in amphibolite without quartz veining.

Modal zonation from biotite- to amphibole rich domains is common. This is particularly vivid around sub horizontal quartz branches associated with alteration type Alt1b and intersecting the amphibolite foliation at locality 5 (Table 2 and Figure 8). The following modal zonation is developed towards the sulphide bearing plagioclase-calcite veins (Figure 8):

Amphibolite with small amount of biotite (host rock)→ Zone1: biotite-plagioclase zone → Zone2: amphibole-plagioclase zone → Zone3: Plagioclase + calcite + apatite zone → Zone3a: pyrrhotite + ilmenite (rutile +titanite) + calcite+ chalcopyrite + apatite ± amphibole in the core of the plagioclase rich Zone3 (Figure 8). A distinctive transition in Ti-bearing phases from ilmenite/ rutile to titanite is observed in the veins (Figure 8). Titanite is the latest Ti-phase given that it always occurs as rims on rutile and Ilmenite. Pyrrhotite and ilmenite formed simultaneously and ilmenite is growing at the expense of rutile because rutile is found as relics included in ilmenite grains (Figure 8).

Biotite bearing alteration rock comparable to those surrounding quartz veins at locality 4 is also common at locality 5 (Alt1d). In some cases the amphibolite mineralogy was replaced by decussate biotite, amphibole, (K-feldspar) and Fe-Ti oxides (Figure 9).

K-feldspar partially replaces biotite (Alt2). In the field this is observed as lighter grey stripes intersecting the dark brown biotite-amphibole rock (Figure 9). Biotite is never completely absent but persists as atoll texture in K-feldspar (Figure 9). Relics of plagioclase occur as cores in K-feldspar or biotite grains.

Quartz veins display a district colour variation which is readily observed in the field and can be correlated with decreasing colour intensity in biotite and amphibole surrounding the veins. Bleached quartz veins are spatially related with zones rich in light green amphibole (tremolite-actinolite), whereas darker and more bluish/pinkish quartz veins are associated with less retrogressed amphibolite. Investigations by Sørensen and Larsen (2007a, paper 1) document, however, that quartz in the quartz veins is related to several stages of dissolution/reprecipitation, meaning that not all quartz in the veins correlate with the surrounding alteration assemblage. Rather quartz vein quartz is partly altered or recrystallised.

Local scapolitisation is common, normally as replacement of plagioclase by scapolite. It is challenging to decide which one of the amphibole types that associates with scapolitisation (Figure 10). Given that the amphibole, plagioclase (Ab65-70An30-33), biotite assemblage is replaced by scapolite; the scapolitisation must by younger than the biotite, amphibole, and plagioclase alteration. Timing of biotite after K-feldspar replacement is also hard to unravel, and they may possibly be simultaneous with the scapolitisation. Large grains of fresh looking biotite are observed in contact with scapolite perhaps implying that biotite and scapolite were in equilibrium (Figure 10). This conclusion is however challenged by grain impingement of scapolite on biotite (Figure 10). Furthermore, country rock amphibolites preserve its dark colour. The scapolite has much higher meionite content than scapolites from elsewhere in the Bamble sector. Relic ilmenite grains are preserved within coronas of first rutile and then titanite which was probably the stable Ti-bearing phase during the scapolitisation and in addition that the reaction cc + ru → ttn + CO_2 occurred in conjunction with the scapolitisation (Figure 10). Scapolite is only observed in places where both calcite and plagioclase are common phases.

Table 2: Main alteration types in amphibolite. See text for discussion.

Alt1: Potassic alteration with biotite stable
Alt1a: Alteration of amphiboles associated with introduction of biotite. Amphibole cores are dark brownish green whereas rims vary from dark bluish green (Amp3a) through light green (Amp3) to almost colour less (Amp4). **Alt1b:** Veins with a central assemblage comprising plagioclase, calcite, apatite, pyrrhotite, ilmenite/rutile and magnesiohornblende (Amp3). Surrounded by two successive alteration zones, the inner zone comprising amphibole, plagioclase and rutile/ilmenite and the outer zone comprising biotite, plagioclase and ilmenite/rutile. **Alt1c**: En-echelon quartz veins intersecting the foliation in the amphibolite, which comprises both biotite, amphibole and plagioclase Biotite-amphibole plagioclase-ilmenite-(pyrrhotite) bearing reaction zones around en echelon quartz veins **Alt1d**: biotite amphibole rock. Titanite most common, but ilmenite preserved as cores together with rutile. Similar to the alteration around the en-echelon quartz veins
Alt2: Potassic alteration K-feldspar replacing plagioclase and biotite
Replacement of biotite by K-feldspar. Final alteration product is a light grey rock consisting of K-feldspar, and light green amphibole (amp4). Titanite is very abundant in this rock type and almost no ilmenite/rutile is observed. Several types of replacements are seen replacing Alt1 assemblages
Alt3: scapolitisation
Massive scapolitisation. Quartz veins surrounded by reaction rim of scapolite, but minor amounts of scapolite are also observed in many places in the amphibolite. The Quartz vein with the reaction rim of scapolite has a different colouration than the quartz vein with less scapolite. The scapolite has a white colour and is only distinguished from commonly occurring white feldspars by its pronounced cleavage

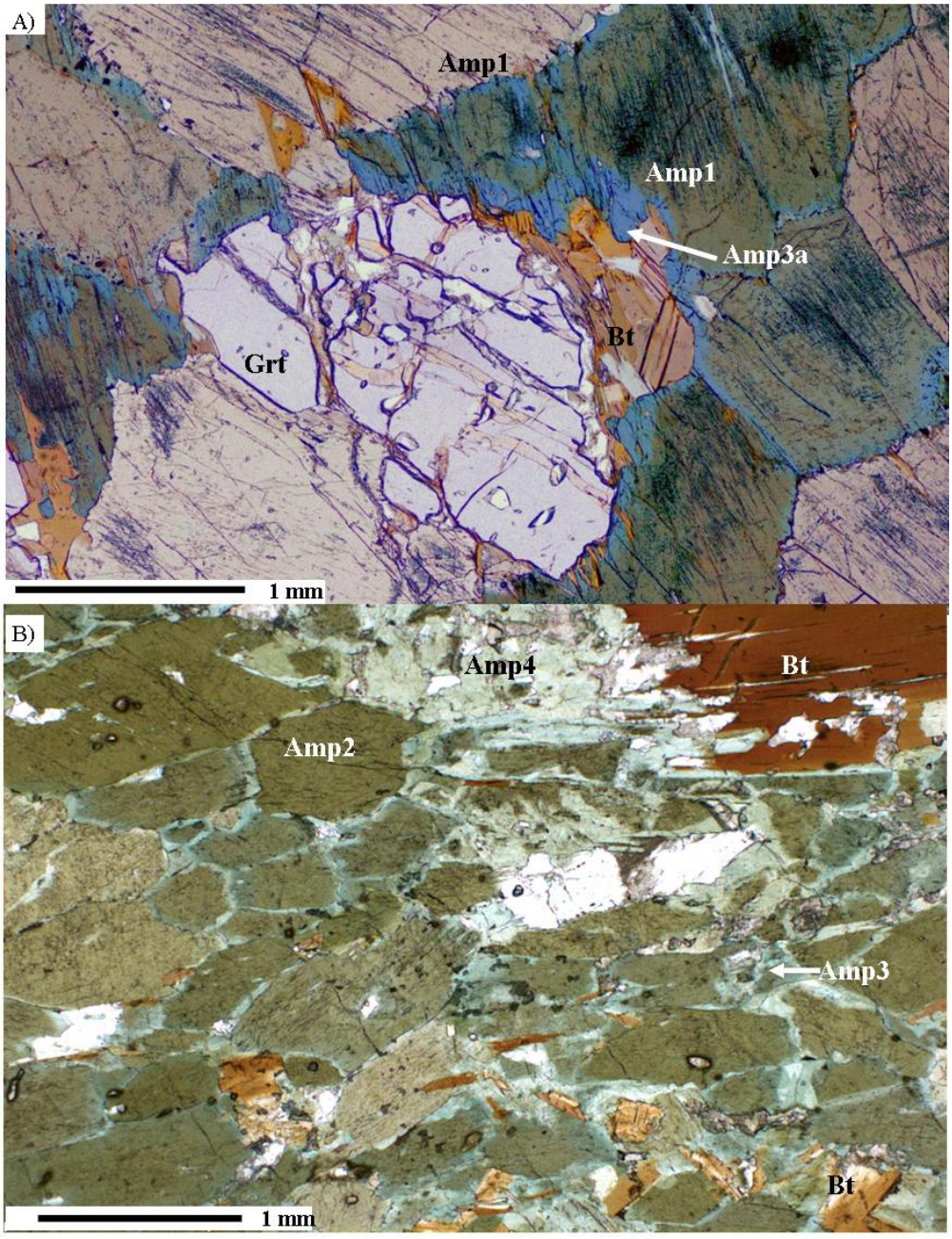

Figure 6: Alteration rims on amphiboles next to biotite grains. A) Amp1 in garnet amphibolite partly altered to Amp3a along cracks and grain boundaries in association with the introduction of biotite. B) Amp2 partly altered to amphiboles types Amp3 and Amp4 along with the formation of biotite.

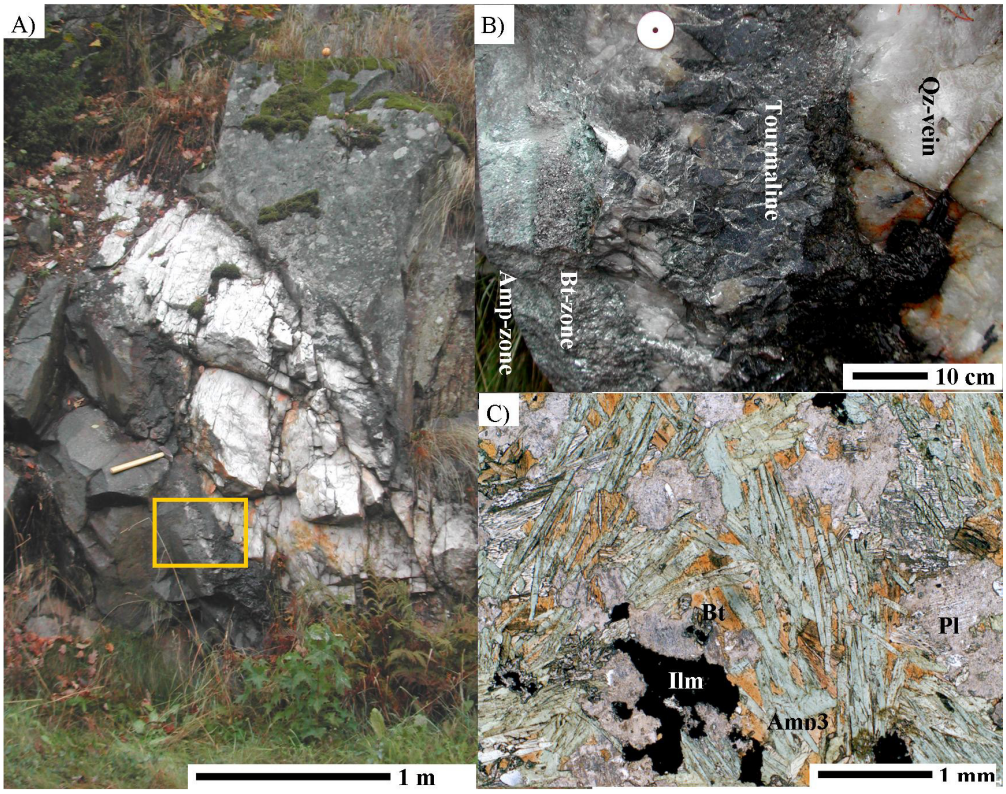

Figure 7: Field appearance and reaction textures around en-echelon quartz veins in amphibolite at locality 4. A) Field image displaying meter thick en echelon quartz vein intersecting amphibolite, yellow box denotes the position of image in B. B) Zoom on the alteration bordering the en echelon veins against the amphibolite. See text for discussion. C) Thin section image showing decussate texture of amphibole and biotite together with ilmenite and dusty plagioclase.

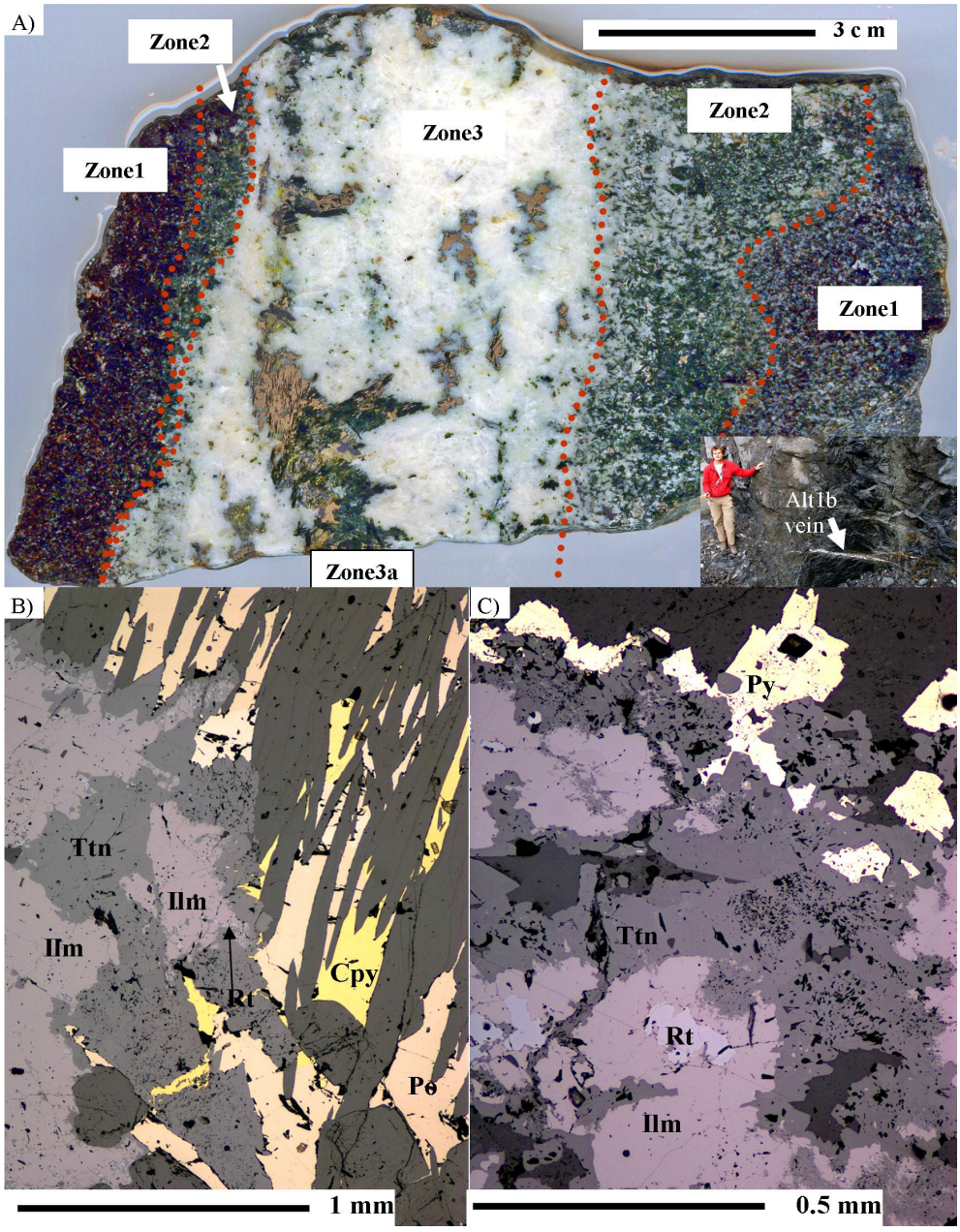

Figure 8: Amphibole plagioclase veins and their textural evolution. A) Note the distinct potassium depletion in the proximal and enrichment in the distal part of the alteration system (see text). Bore mineral assemblage in amphibole Amp3. C) Successive changes in Ti-phase stability.

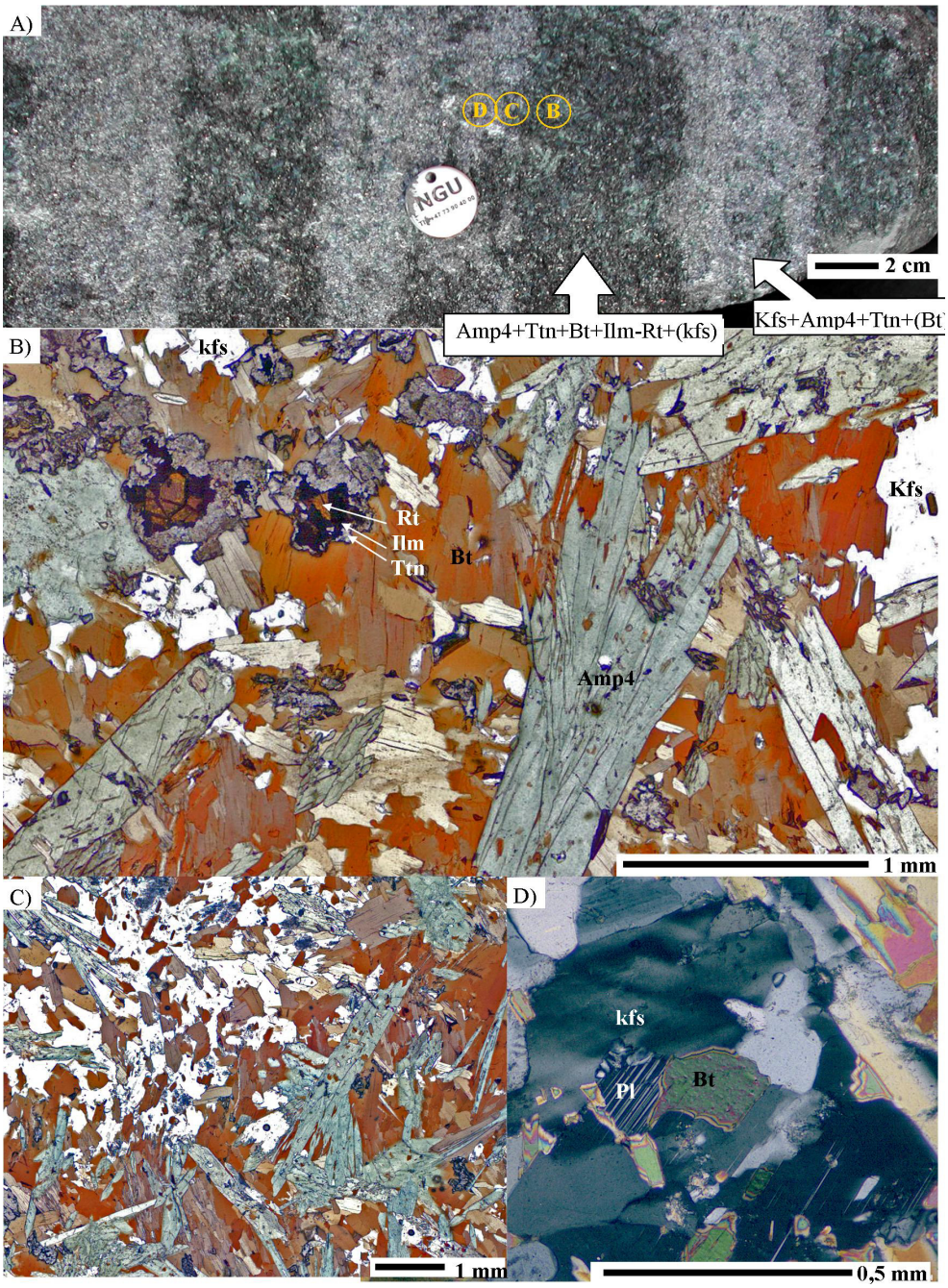

Figure 9: Decussate texture of biotite, amphiboles and Fe-Ti phases partly replaced by K-feldspar, amphibole titanite assemblage. A) Field image of fingering replacement pattern of the grey K-feldspar bearing rock on the Amphibole biotite rock. B) Decussate texture

of amphibole, and minor K-feldspar. Note the successive change in Ti-bearing from cores of rutile through ilmenite to titanite. C) K-feldspar replacing biotite, with left over grains of biotite inside the K-feldspar grains giving an atoll texture. Note that there is no ilmenite in the K-feldspar rich domain D) Remnants of plagioclase inside K-feldspar grain.

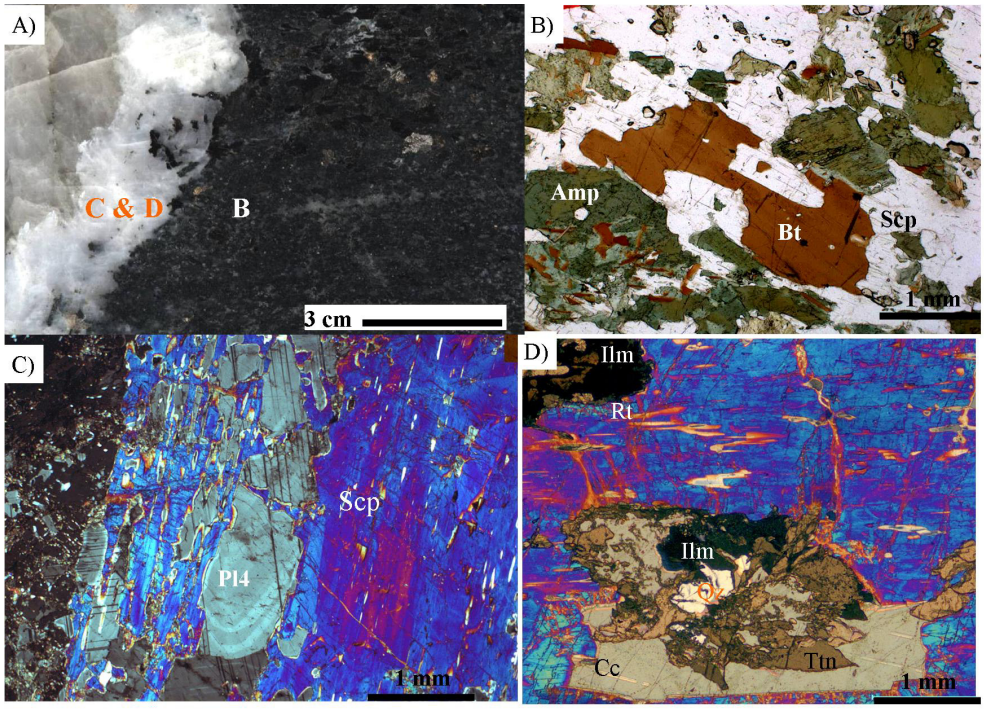

Figure 10: Scapolitisation observed around quartz-scapolite vein. A) Polished slab with indication of thin section images. From right to left is first grey quartz, followed by white scapolite and then scapolitised amphibolite. B) Scapolitised amphibolite. C) Scapolite replacing plagioclase intersecting growth zoning and deformation twins. D) Calcite ilmenite, rutile and quartz reacting to form titanite.

4.2 Mineral chemistry

EPMA was done with a JEOL JXA-8900 M combined WDS-EDS microprobe at the department of Materials Science NTNU. Results were standardised using a ZAF correction for matrix effects. Biotite, muscovite, amphibole, plagioclase and epidote data were collected using the same standard setup (Table 3). Apatite analyses were calibrated with an apatite standard, except for F and Cl where fluorite and tugtupite standards respectively were used because F and Cl may migrate through the atomic lattice of apatite as a result of electron bombardment (Table 3). Amphibole formulae were calculated estimating Fe^{3+} from cation occupancy and charge balance with 13

Cnk for amphiboles. Accordingly, Fe^{3+} value of the calcic amphiboles is a stoichiometric estimate and not a measured value. However, comparisons of measured and calculated Fe^{3+} in calcic amphiboles show that the 13 Cnk method is the most accurate (e.g. Cosca et al., 1991; Gualda and Vlach, 2005). Scapolite formula was recalculated with the procedure of Teertstra and co-workers (1997), with an additional iterative procedure to estimate HCO_3 and CO_3 (see section 4.2.2). Biotite mica was normalised to 22 oxygen, apatite to 25 oxygen, feldspar to 32 oxygen with all Fe assumed to be Fe^{2+}. The quality of Na, Ca and Al analyses was attained by comparing calculated feldspar formulas with the ideal stoichiometry of feldspar using the relation , NaK(1-Ca)Ca(Ca)Al(1+Ca)Si(3-Ca)O8. This gave satisfying results with deviation within 0-2 % of the ideal values.

Table 3: Standards used in calibration of EPMA analysis

element	Silicate setup	Apatite setup
Si	Wollastonite	Wollastonite
Al	Spessartine garnet	Spessartine garnet
Ti	Titanite	Titanite
Fe	Olivine	Olivine
Mg	Olivine	Olivine
Mn	Spessartine garnet	Spessartine garnet
Ca	Wollastonite	Apatite
Na	Albite	Albite
K	Orthoclase	Orthoclase
P	Apatite	Apatite
Cr	Chromite	Chromite
V	Element standard	Element standard
F	CaF	CaF
Cl	Tugtupite	Tugtupite

4.2.1 Amphiboles and biotites

Figure 11 show the general geochemical evolution of the amphiboles vs. their Si content. Geochemical trends of amphibole cores and rims are strongly contrasting (Figure 11). Amphibole cores follow their own trend whereas the amphibole rims are aligned along a single geochemical trend (Figure 11). Particularly, this is evident in the plot displaying Al^{VI}+Fe3++Ti vs. Si (Figure 11). Both prograde and retrograde trends in amphiboles are observed (Figure 11).

The prograde evolution of amphibole in garnet amphibolite follows trends from ferri-tschermakitic toward hastingsitic to ferropargasitic compositions (Figure 11). The main exchange vector during prograde conditions is substitution of Fe^{2+} for Fe^{3+}. The total amount of Fe recorded by zonings in amphibole types 1, 1a, and 2 is constant within each amphibole and changes in Fe^{3+} and Fe^{2+} only reflects the $Fe^{2+} \Leftrightarrow Fe^{3+}$ substitution.

In a Fe^{2+} vs. Fe^{3+} diagram a set of lines with inclination -1 arise but with differing intercepts (Figure 12). A main charge compensating substitutions is Na for Ca at the M4-site and (Na,K) for vacancy (□) in A, which have a linear correlations with the Fe^{3+} content (Figure 12). Although compensating substitutions have a good linear correlation they are not explaining the total charge balance given that substituting mol fraction is 0.62 and not 1 as required. Probably, the missing charges may be accounted for by oxy-substitution, i.e. the amphiboles were partially oxidized with O_2^- substituting for OH^- as also documented in experiments under H^+ deficient conditions (Clowe et al., 1988; Popp et al., 1995). However, given the stoichiometric approach to the Fe3+ estimate, this conclusion is uncertain. Only tschermakitic amphiboles in the garnet amphibolite have considerable Fe^{3+} contents whereas amphibole cores in the garnet-free amphibolite has low Fe^{3+} contents and high Fe^{2+} contents. Amp1 show coupled increase in A-site occupancy and decreasing X_{Mg} (Figure 11). The other core type amphiboles are relatively enriched in Cl and (Na, K) in the A-site compared to the retrograde overgrowth rims (Figure 11).

Retrograde overgrowths rims on amphiboles show a wide range of compositions, from ferro-tschermakite /tschermakite towards actinolite in a trend going along the ferro-pargasite exchange vector toward actinolite with XMg ≈ 0.9(Figure 11). With increasing X_{Mg} and Si content they are progressively depleted in Cl and (Na, K) in A. The relation between Fe^{2+} and Fe^{3+} is less systematic. This reflects variations in the Fe_{tot} and the Fe^{2+}/Fe^{3+} ratio. The main factor in this trend is a drop in Fe_{tot}, whereas the Fe^{3+} contents generally are low (Figure 11).

Along with the increasing X_{Mg} and Si contents the total amount of tetra- and trivalent ions in the M sites also decreases along a linear trend, which is not followed by amphibole cores (Figure 11). A plot of Al^{VI} against Si does not show as strong a correlation as the former, and additionally show disarrays for the core type amphiboles (not shown). This imply that even low concentrations of Fe^{3+} influence the Al^{VI} substitution mechanisms in the retrograde overgrowth rims and retrograde amphiboles.

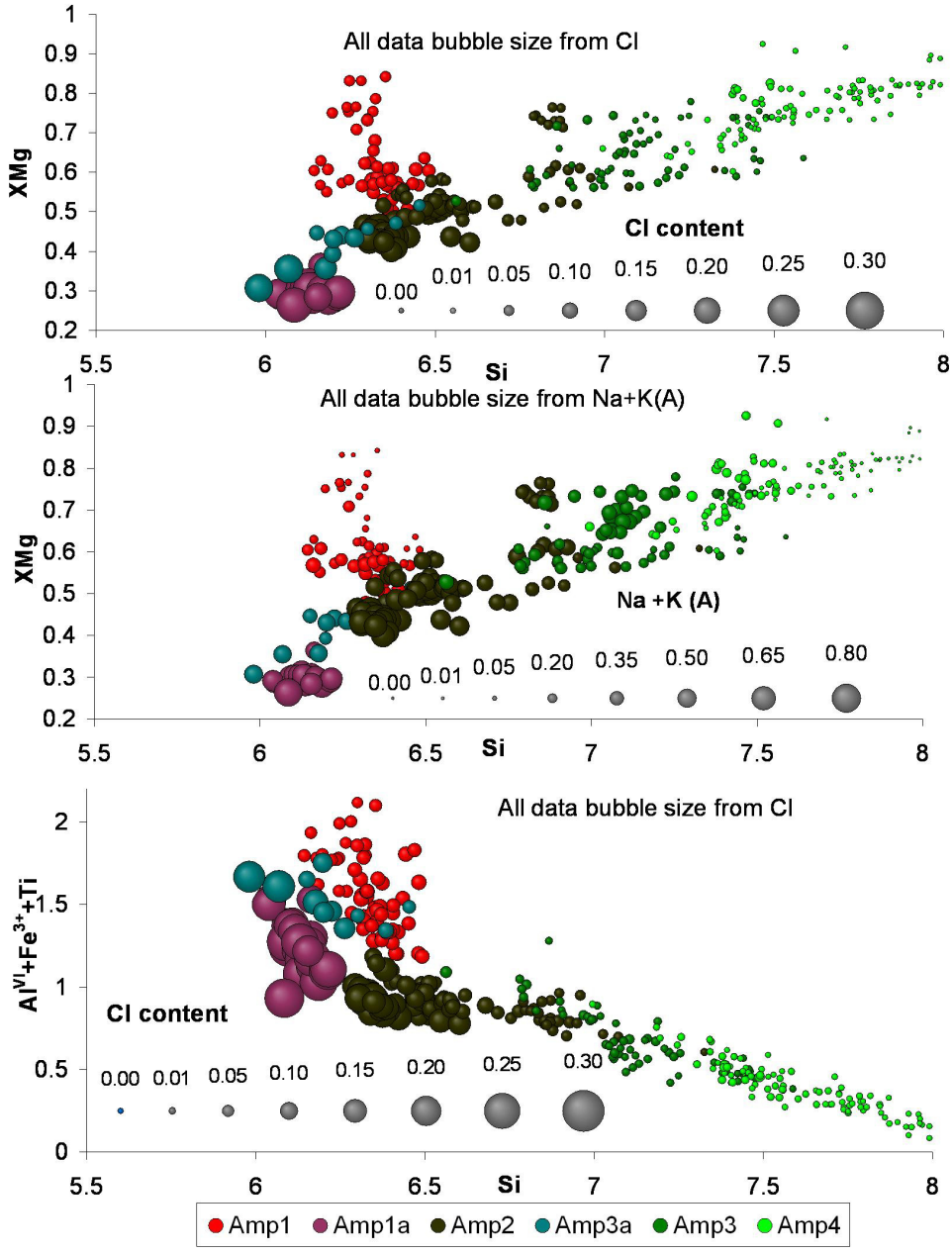

Figure 11: General amphibole evolution. Upper two diagrams displays the evolution in X_{Mg} versus Si plot, show the interdependence between X_{Mg}(Mg/(Mg+Fe^{2+}), Si, (Na, K)) in A and Cl. Note that this plot corresponds to the plotting scheme of Leake et al. (1997).

Lowermost diagram shows the evolution in terms of octahedral Al, Fe3+ and Ti and Cl. See text for discussion

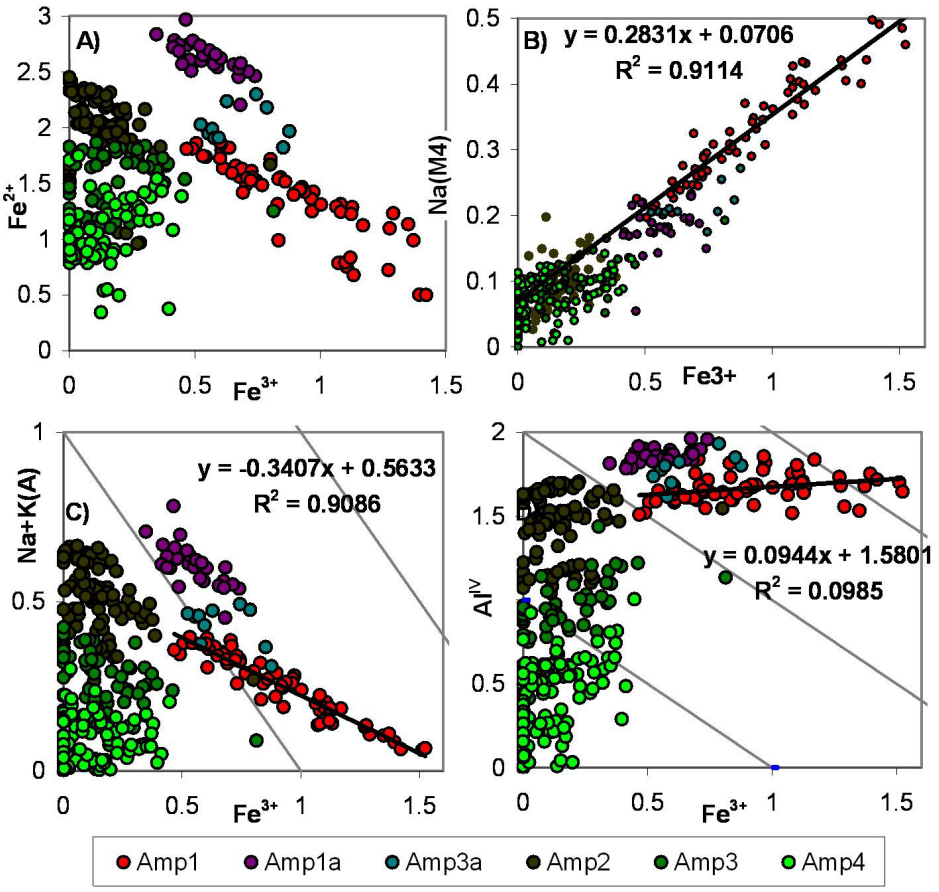

Figure 12: Trends with Fe^{3+}, regression lines based on amp1 data only. A) Fe^{2+}vs. Fe^{3+} B) Na(M4) vs. Fe^{3+}C) Na +K (A) vs. Fe^{3+}D) Al^{IV} vs. Fe^{3+}. Note grey lines marking 1:1 correlations for comparison. See text for discussion.

All amphiboles except Amp1 show correlations of several other elements with their Cl-content (Figure 13). In Amp1 the only correlation that was found was a positive correlation between Fe^{2+} and Cl (Figure 13). The trends vary between the amphibole types in both inclination and intercepts (Figure 13). Trends between K and Cl display different linear correlations for the individual amphibole groups (Figure 13). The inclination of trends of K vs. Cl in Amp1a and Amp2 are similar but they have different intercepts (Figure 13). With respect to the amphiboles that coexist with biotite

(Amp3 and Amp4), trends vary between locality 1 and 5. The blue-green amphibole rims (Amp3a) show a flat trend whereas the retrograde overgrowths at locality 5 show a step trend for both Amp3 and Amp4 (Figure 13).

X_{Mg} and Fe contents also correlate with Cl. The X_{Mg} for all data, except Amp1 fits on a linear trend with an inclination of -2. Amp1, however, follows a steep trend with an inclination of about -7. In approaching the detection limit for Cl Amp3 and Amp4 should not follow distinctive trends for this element. However a zoom on the plot suggest that the low Cl concentration data separates into two strictly linear and parallel trends (Figure 13). Possibly, this difference in intercept reflects contrasting Fe_{tot} in the geochemical system (i.e. the protholith). This is reflected by the two groups of the core amphiboles Amp2, with different Fe_{tot} (Figure 13c). Similar effects are also observed with respect to X_{Mg}.

Fe_{tot} in Amp1, Amp1a and Amp2 varies independently of their Cl contents (Figure 13c). The Fe_{tot} within amphibole types Amp1, Amp1a and Amp2 is not affected by the Cl incorporation although there is a general grouping with high Fe_{tot} amphiboles having higher Cl (Figure 13). Contrary to Fe_{tot}, both Fe^{2+} hence also X_{Mg} correlates with Cl in Amp1, whereas there is no correlation in Amp1a and Amp2 except for the general tendency for amphiboles with high Fe content to be more Cl rich as observed with Fe_{tot}. Accordingly, in Amp1a and Amp2 the incorporation of Cl mostly affect the K content (Figure 13a), whereas high Fe-contents probably promotes Cl incorporation (Figure 13b-d). A similar effect is seen in the Al^{IV}/Si content for Amp1, Amp1a and Amp2 although it is more clear with respect to Fe_{tot} (Figure 13e).

The overall Froland trends in the amphiboles are realised in single grains (Figure 14). Overgrowths of Amp3 and Amp4 are observed on Amp2 and overgrowths of Amp4 on Amp3 are commonly observed. In all cases the chemical change from core to rim is the same, following the general trends with increasing Mg and Si and decreasing Fe, Al^{IV}, Al^{VI}, Cl., Ti, K and Cl (Figure 14).

Amphibole chemistry in the other characteristic alteration types also follows the systematic evolution demonstrated by the biotite-related amphibole rims. Amphiboles in early biotite potassic alteration types Alt11b-c are magnesiohornblende (Amp3), whereas amphiboles in the K-feldspar bearing potassic alteration assemblages are more actinolitic and belong to the Amp4 group.

Because Amp3, Amp3a and Amp4 in mostly correlated petrographically with biotite it is usefull to compare coexisting amphibole and biotite. As for the amphiboles, the Cl content of biotite correlates negatively with X_{Mg} and positively with the Fe content (Figure 15). There are curvilinear correlations between the X_{Mg} and Fe, Mg and Cl-contents of coexisting amphibole and biotite (Figure 15). The Cl content of biotite is generally higher than that of coexisting amphibole, but at high Cl contents, the Cl contents of amphibole and biotite are similar (Figure 15). Only poor correlations are found between Al^{IV} and Cl content of biotite and between the Al^{IV} of biotite/amphibole pairs (Figure 15).

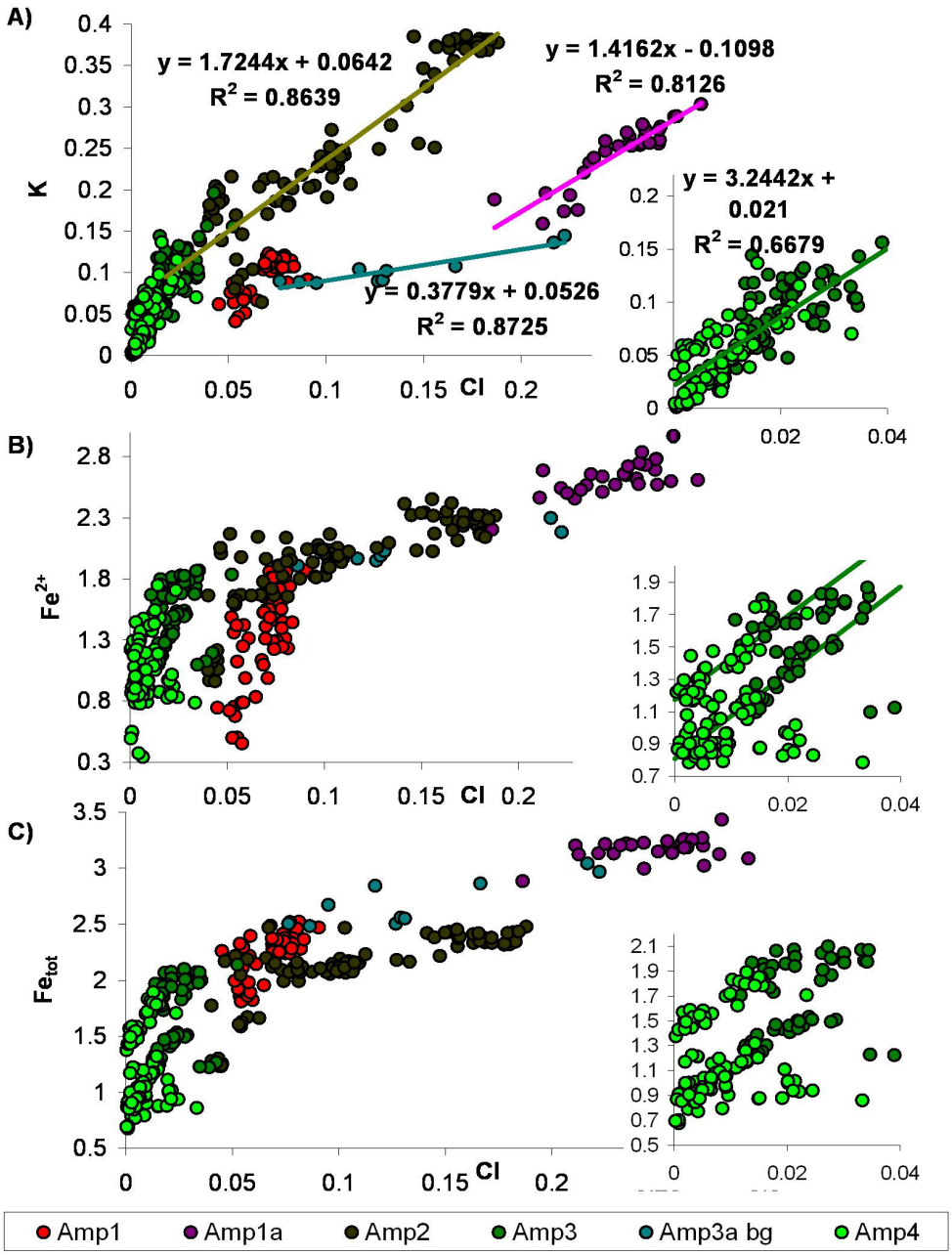

Figure 13: Composition of amphibole as a function of Cl-content. A) K vs. Cl B) Fe2+ vs. Cl C) Fe_{tot} vs. Cl. D) XMg vs. Cl. E) Al^{IV} See text for discussion. F) Al^{VI} vs. Cl. See text for discussion.

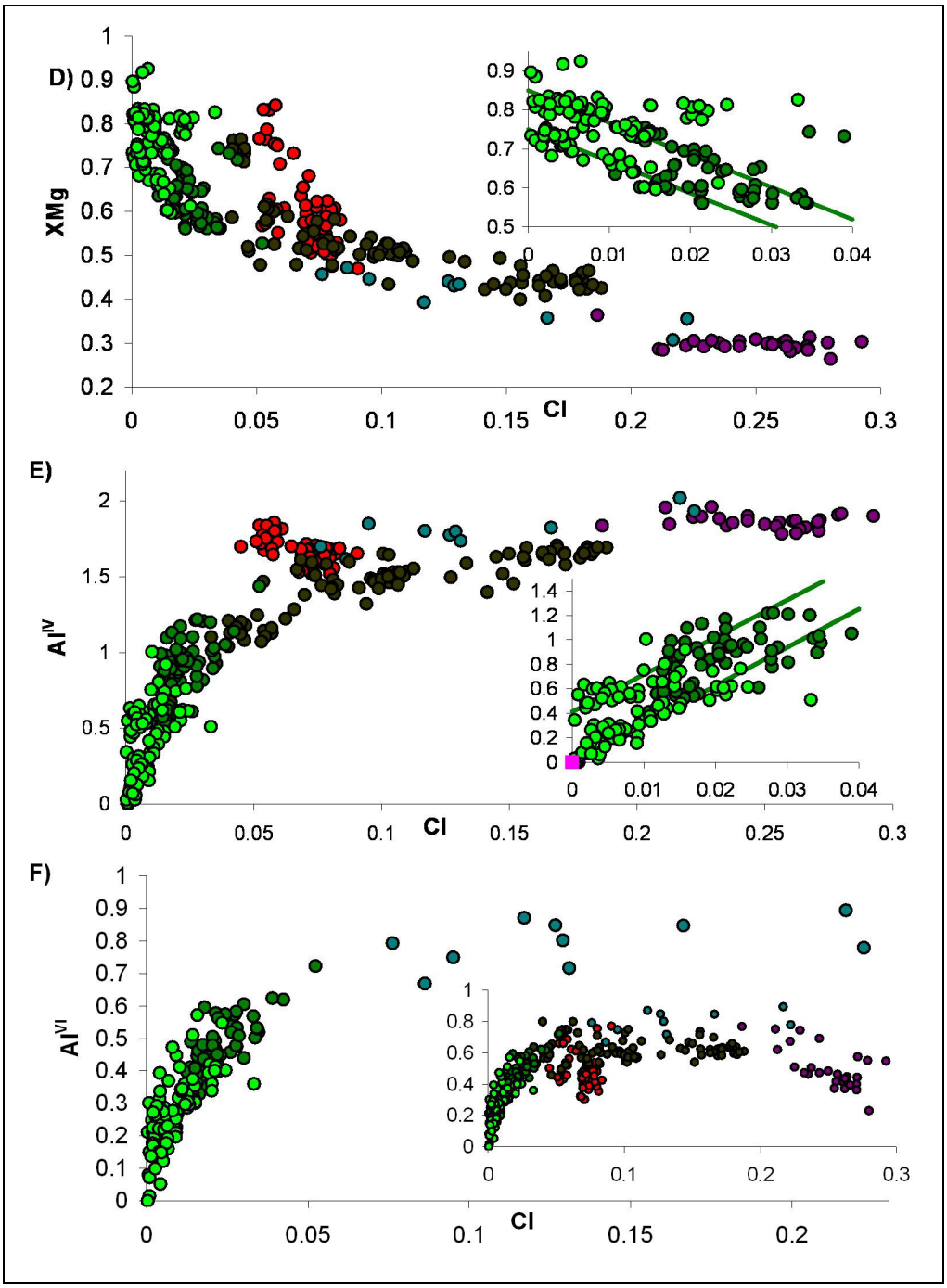

Figure 13 (continued), caption on previous page.

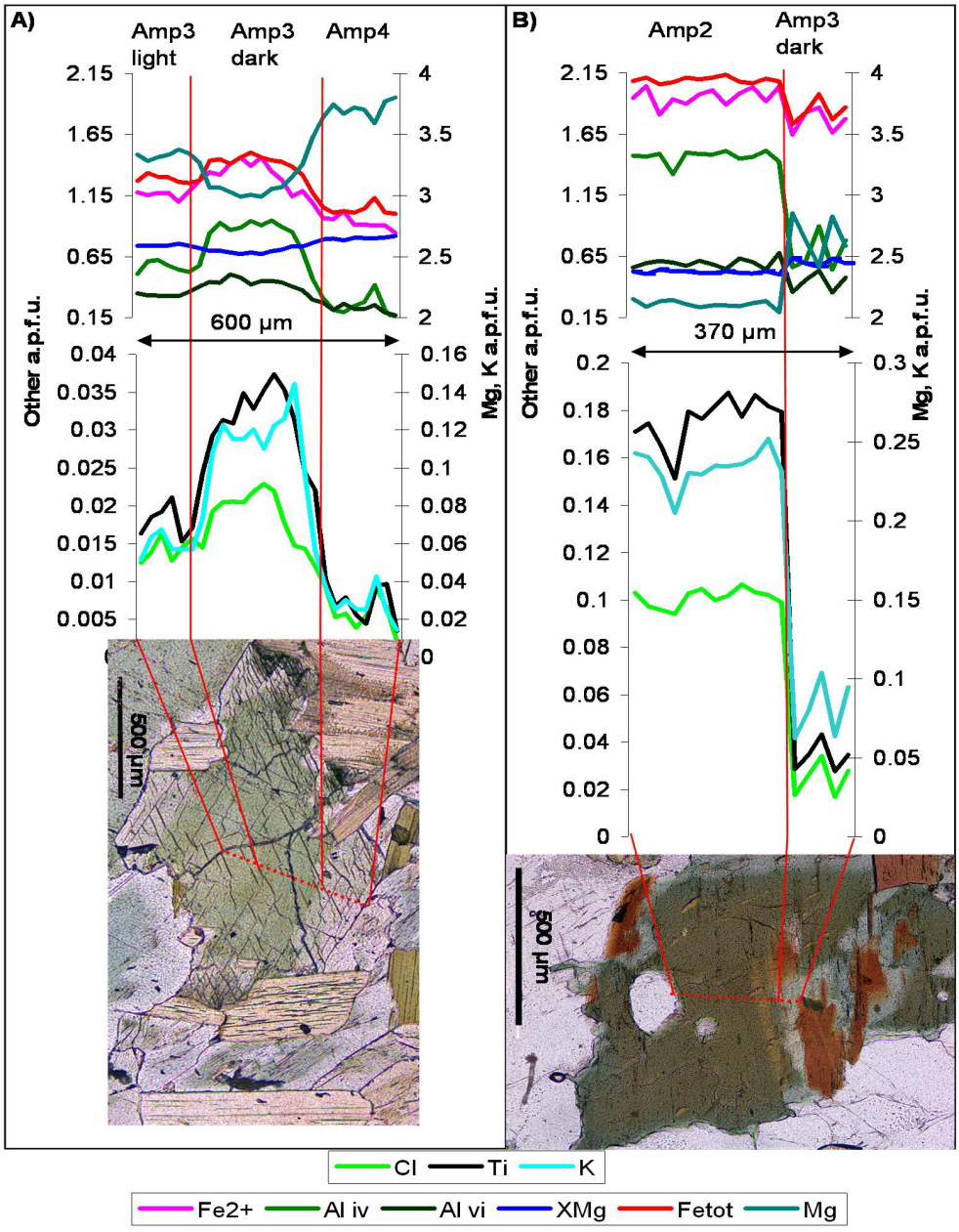

Figure 14: Line scans across amphibole grains showing the stages in the progressive amphibole alteration. A) Amp3 partly altered to Amp4. Note that biotite is in contact with both types. B) Overgrowth of Amp3 on Amp2. Note the sharp alteration boundary when compared to A., Both amphiboles are from locality 5.

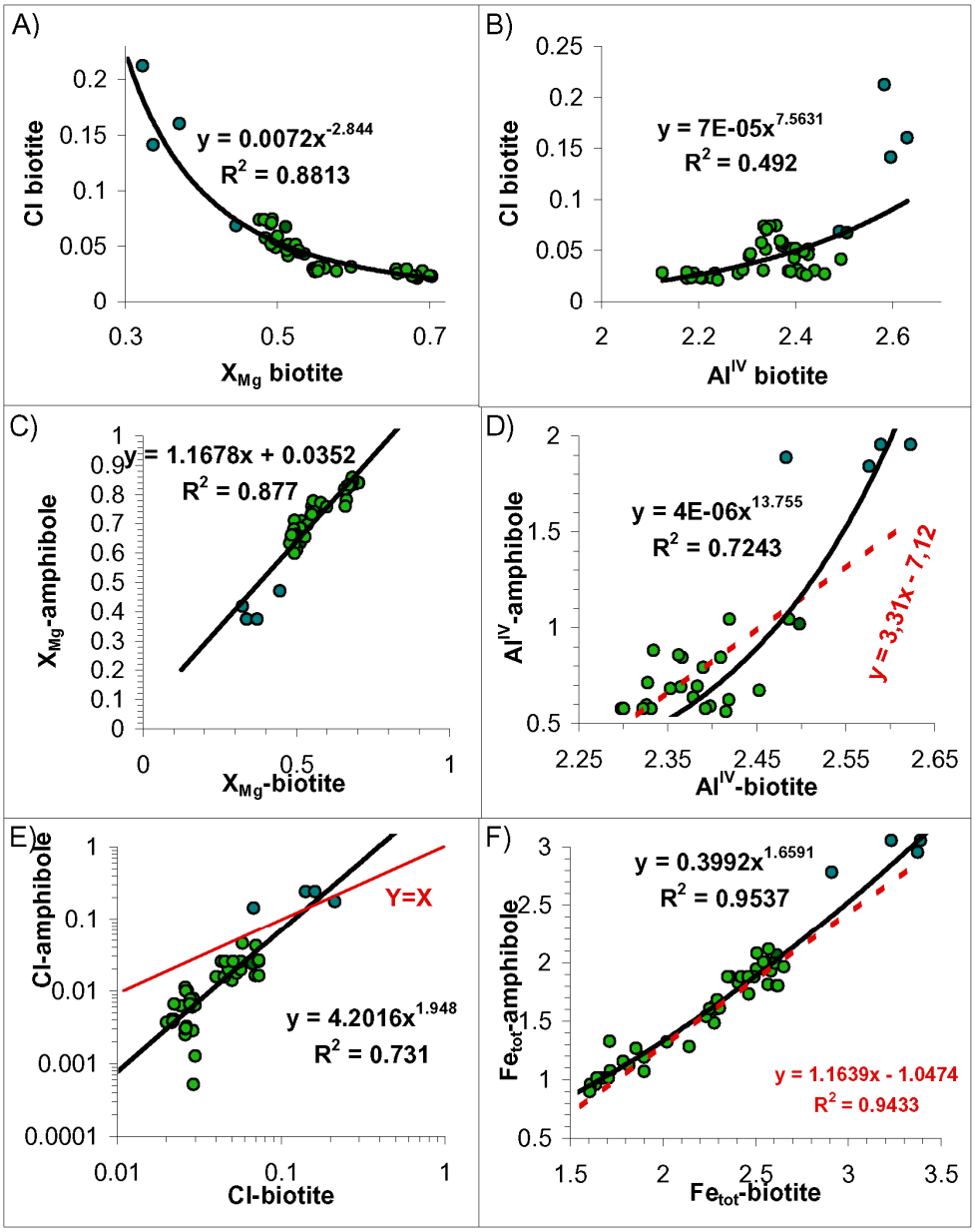

Figure 15: Comparison of biotite and amphibole evolution. A) The Cl content of biotite against the XMg of biotite, with a power law correlation. B) Al^{VI} content and Cl of biotite only display a weak correlation. C) Correlation between X_{Mg} of coexisting amphibole and biotite. D) Al^{VI} of coexisting amphibole and biotite only display a weak correlation. E) Correlation between Cl-contents of coexisting amphibole and biotite. F) Correlations

between Fe_{tot} in coexisting amphibole and biotite. Colour labelling of amphibole same as in Figure 11,12 and 13.

4.2.2 Plagioclase and scapolite

The composition of plagioclase varies amongst the localities and plagioclase also evolves toward higher albite contents as amphibolite alteration proceeds. Plagioclase in garnet amphibolite (Pl1) has a restricted compositional range ($An_{39.4}Ab_{60.4}Or_{0.2}$). Pl1 is unzoned, however, is overgrown by albite rich plagioclase (Pl1-rim $An_{30,1}Ab_{69,8}Or_{0,1}$). The garnet quartz symplectites have one group of plagioclases having the same composition as Pl1(Pl3) in the garnet amphibolite and also comprise an albite rich plagioclase (Pl3a).

Plagioclase texturally correlated with amphibole cores in the garnet free amphibolite (locality 5), is considerably more Anorthite rich ($An_{51,4}Ab_{47,9}Or_{0,8}$) than plagioclase in the garnet amphibolite. Secondary plagioclase is more albite rich, but divides in two main groups i.e. Pl3 ($An_{37,3\text{-}45,3}Ab_{53,9\text{-}61,9}Or_{0,2\text{-}1,4}$) and Pl4 ($An_{28,9\text{-}33,4}Ab_{65,7\text{-}70,3}Or_{0,6\text{-}1,0}$). Pl3 is associated with Alt4, whereas plagioclase Pl4 replaces Pl3, but probably also coexist with the amphibole-biotite assemblages.

Table 4: Representative plagioclase analyses. Note to few analyse of pl1-rims for statistics

Type	averaged values			range		
	An	Ab	Or	An	Ab	Or
Pl1	39,4±0,8	60,3±0,8	0,3±0,1	37,6-40,9	58,8-62,2	0,2-0,4
Pl2	51,4±0,7	47,9±0,8	0,8±0,1	50,5-53,3	46,0-48,8	0,6-0,9
Pl3	40,4±2,3	58,8±2,2	0,8±0,2	37,3-45,3	53,9-61,9	0,2-1,4
Pl4	30,5±1,3	68,6±1,3	0,8±0,1	28,9-33,4	65,7-70,3	0,6-1,0
Pl1-rims	30,1	69,8	0,1	?	?	?
Pl3a	20,0±3,2	79,6±3,3	0,4±0,2	16,3-23,3	76,1-83,4	0,2-0,7

Scapolite was only documented in samples from locality 5. It replaces both the primary and the secondary plagioclases. The stoichiometric formula of scapolite is of the form (e.g. Teertstra and Sheriff, 1997):

$M_4T_{12}O_{24}A$, where M= Ca, Na, K; T= Si, Al; A= Cl, CO_3, SO_4, HCO_3 and OH

All analyses are close to ideal stoichiometry with 12 Si and Al and approximately 4 cations in the M site. Scapolite in the area shows considerable compositional variation (EqAn=100*(Al-3)/3=41.3-59.5). The scapolite has a significant Cl content, whereas S

and F only occur in minor amounts. The Cl and Na content have negative linear correlations with EqAn, whereas the sum of divalent cations (≈Ca) has a positive correlation (Figure 16). The K content on the contrary, shows a positive although poor correlation with EqAn (Figure 16).

CO_3^{2-} was estimated using 3 model calculations: 1. Charge balance optimisation using $\Sigma M+=\Sigma A^{-}+\Sigma TO2^{-}$ (see Teertstra and Sheriff, 1997) 2: A-site occupancy (CO_3=1-S-Cl-F) 3. Combined charge balance and A-site occupancy by an iterative method, gives a result that can be caused by both OH^- and HCO_3^-. Method 2 gives a systematic correlation between A-site occupancy and EqAn (Figure 17). The correlation with EqAn is inherited from the correlation between Cl and EqAn, and this model satisfies charge balance constraints but not site occupancy. Method 1 gives a poor correlation between EqAn and the CO_3 content (Figure 17). Model 3 provides the best fit as it charge balance A-site occupancy and is correlated with EqAn (Figure 17). The modelling suggests that other species than CO_3^{2-} and Cl^- is present in the scapolite. We suggest that they are water related species i.e. OH^- and HCO_3, but cannot prove it because this would require a quantitative estimate of the water content.

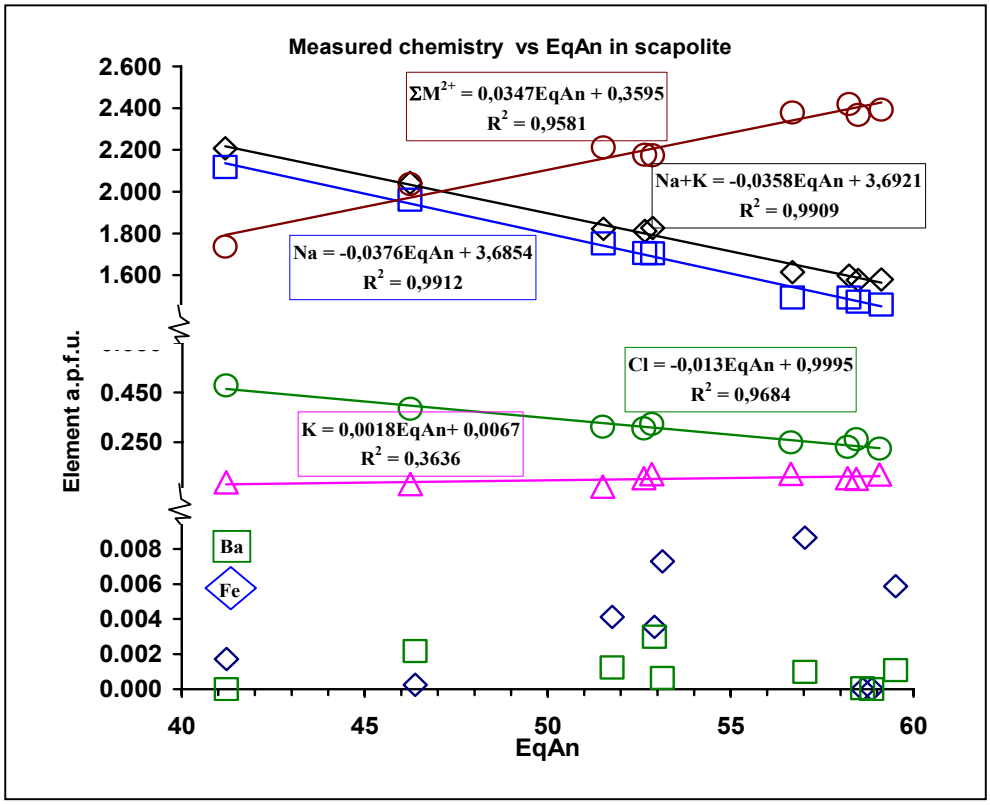

Figure 16: Scapolite chemistry in element a.p.f.u. vs EqAn (100*(Al-3)/3). See text for discussion.

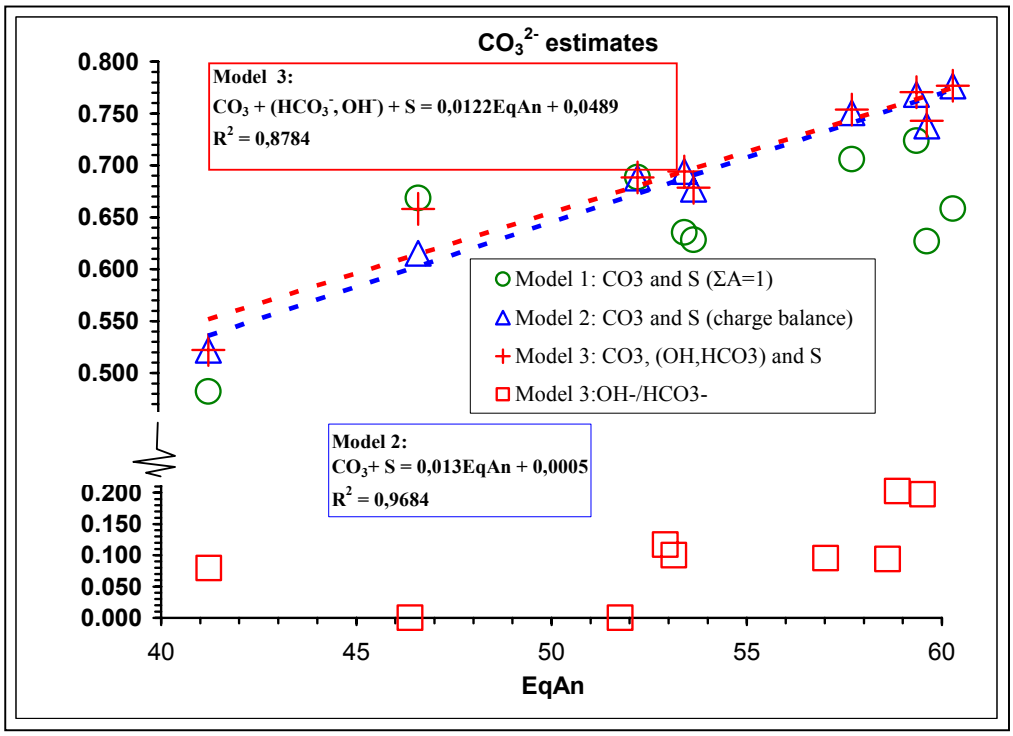

Figure 17: The three models of CO_3 estimation, only model 2 and 3 give reasonable correlations between CO_3 and EqAn. Model 3 was preferred for calculations of endmembers and exchange vectors because it gives better correlation in the dataset. See text for discussion

4.2.3 Apatite

Apatite also follows a systematic evolution in their halogen geochemistry. The evolution path of apatite, however, deviates significantly from the paths of biotites and amphiboles. Apatite contains considerable amounts of F not detected in amphibole and biotite. Apatite in garnet quartz symplectites is Cl-apatite. Apatite coexisting with the alteration assemblages show rising F with increasing degrees of alteration in samples where amphibole and biotite are more Mg-rich and poor in Cl, Al and Fe (Figure 18). Early apatite in garnet quartz symplectites is relatively enriched in Ce, which is incorporated in monazite next to altered Cl-apatite grains (Figure 18). Late F-apatite coexisting with Amp4 display enrichment in Ce and Y, whereas intermediate apatite coexisting with Amp3 is not enriched in neither Ce nor Y (Figure 18).

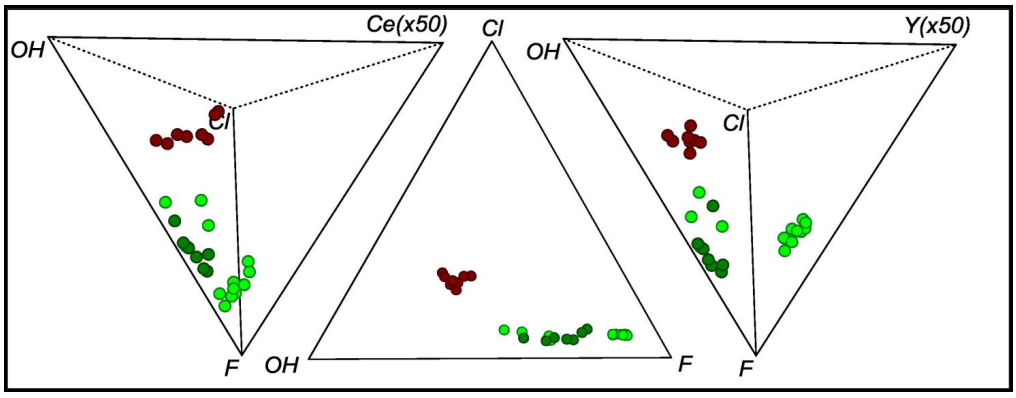

Figure 18: Halogens in apatite. Dark red brown is apatite in garnet quartz symplectites co-existing with Amp1a. Green symbols represent apatite occurring together with Amp3 and light green occurring together with amp 4. Middle diagram display the halogen evolution, diagram to the left the coupling with the Ce-content and the diagram to the right the Y- content. See text for discussion.

5 Discussion

This paper documents a well defined retrogression path for the amphiboles. The aim of this discussion is to relate the amphibole evolutions to the fluid evolution of the Bamble shear zone. The chemical evolutions of the hydrous phases confirm and complement the results of fluid inclusion analysis by Sørensen and Larsen (2007b, paper 2).

The chemical evolution of amphibole is stored in its halogen make up. In the following sections we will document how halogen chemistry changes in the amphiboles relates to the fluid properties and metamorphic conditions. The aim is also to approach the source and regional origin of metasomatism in the Froland area as well as the Bamble zone.

5.1 Prograde-retrograde evolution of amphibolite

The garnet amphibolite amphiboles follow a different chemical trend when compared to other amphibole types when looking at variations in Fe^{3+}, Na(M4) and (Na,K) in A. Furthermore, charge balance constraints suggest that the amphiboles were oxidised during a period of low fH^{+}. However, field evidence show that the garnet amphibolite formed as a result of hydration of the hyperite with a gradual transition from coronitic gabbro to pyroxene free garnet amphibolite. As this hydration process is not in agreement with low fH^{+} (e.g. Clowe et al., 1988) we infer that the garnet amphibolite was subjected to oxidation after initial amphibolitisation. The correlation between decreasing XMg, Fe^{3+} and Cl suggests that amphiboles in the garnet amphibolite partially equilibrated to the fugacity conditions of an infiltrating chloride

bearing fluid. This may reflect the conditions at which Amp2 in the garnet free amphibolite formed.

1. To summarise, the amphibolites went through the following evolutionary stages:
2. Amphibolitisation of gabbro
3. Cessation in amphibolitisation and oxidation of amphiboles in garnet amphibolite during H^+ deficient conditions
4. High-grade amphibolite facies alteration and amphibolitisation under the influence of chloride bearing solutions
5. Biotite stabilised in the amphibolites (Alt1), due to infiltrating K-bearing brines with near constant salinity. Amphiboles react with the infiltrating fluid causing changes in amphibole composition. The most common expression of the fluid infiltration is overgrowth rims on amphiboles against introduced biotite grains. In zones of more intense alteration more complex alteration develops.
6. Stabilisation of K-feldspar at the expense of biotite and plagioclase (Alt2).
7. High fH_2O destabilises calcite and the assemblage calcite+ (ilmenite)/rutile + quartz which is replaced by the assemblage titanite + CO_2. This leaves CO_2 available for the formation of rather meionite rich scapolite according to the simple reaction; plagioclase+CO_2+NaCl+ Ca(Aq) → Scapolite+ quartz (Alt3). As no trace of CO_2 was detected in the coexisting fluid inclusions (paper 2, Sørensen and Larsen, 2007b), it is assumed that the CO_2 in the scapolite must be locally derived i.e. from decomposition of calcite and that the CO_2 did not mix into the aqueous brine. This also document that scapolite formed below the PT conditions of the solvus in the H_2O-CO_2-salt system hence also why scapolite is only observed in association with calcite.

5.2 Cl-OH in amphibole and biotite during retrogression

The Cl content of amphibole and biotite is a function of several factors including pressure, temperature, fluid composition and the actual composition of the amphibole that partially is a function of the host rock chemistry. These effects are probably reflected in our data. The effect of the amphibole chemistry is reflected by the shift in K vs. Cl contents trends of amphiboles with different Fe_{tot} content. Cores of amphibole follow individual trends at each locality whereas rims follow a general trend. In both retrograde amphiboles and in biotite there is a negative correlation between X_{Mg} and Cl. Biotite features a linear correlation between X_{Mg} and $\log(OH_{biotite}/Cl_{biotite})$.

(Munoz, 1992; Munoz and Swenson, 1981) suggested that the Cl-content of biotite is a function of the Mg-Cl avoidance effect and the original Fe/Mg ratio at given PT-Xfluid condition. However, calculated f_{H_2O}/f_{HCl} using Munoz (1992) produces a linear correlation with X_{Mg} in biotite irrespective of the temperature, thus suggesting that fluid composition varied (not shown). Contrary to this conclusion, the studies of

Sørensen and Larsen (2007b) suggest near constant salinity in the fluid and show that potassic alteration took place in the temperature interval c. 625-450°C. Biotite also formed in this T-interval. It is not possible to obtain the observed variation in biotite Cl content using a constant fluid Cl/OH ratio and the Mg-Cl avoidance model suggested by (Munoz, 1992; Munoz and Swenson, 1981).

In agreement with Kullerud (2000) we suggest that the disagreement is a result of uncertainties in the assumptions made by Munoz and co-workers in their Mg-Cl avoidance models. The Cl-Mg avoidance model rest on the argument that linear trends between log(XF/XCl) and XMg in biotite imply constant PT-Xfluid conditions and that the Cl-content was controlled by the Mg-Fe ratio of biotite. This is a strongly biased opinion given that, thermodynamically, there may be several other explanations for univariant trends. The controlling parameter can not be decided alone from the univariant trend. Many parameters could be involved including the PT-conditions, fluid composition, chemical potentials and internal chemical constraints.

Also opposing the Mg-Cl avoidance model of Munoz and co-workers is that both the Froland amphiboles and biotites feature rim ward increase in XMg. This suggests that XMg in both minerals was controlled by an external parameter. As other phases also become lower in Fe, the only interpretation is metasomatism, i.e. Fe was mobilised and depleted from the amphibolites. The question is what induces this metasomatism. Zoned amphiboles in other studies have been related to changes in fluid composition at fixed PT in both metamorphic (e.g. Kullerud, 1995; Kullerud, 1996; Kullerud and Erambert, 1999; Kullerud et al., 2000; Xiao et al., 2005) and magmatic (Sato et al., 2005) environments. However, in Froland the fluids maintained constant Cl/H_2O ratios throughout cooling and uplift (Sørensen and Larsen(2007b, paper 2). Accordingly, this is not the underlying cause of Mg-zonation.

Kullerud (2000) argue that gradual changes in PT conditions with fluids of fixed Cl/H_2O ratios would produce similar trends. That is also the most likely explanation for the Froland amphiboles. The key to understand the linear trends lie in the relation between coexisting biotite and amphibole, which also are univariantly correlated along logarithmic trends. The K_DFe between biotite and amphibole may be expressed in the following way (e.g. Cooper (1972)):

$$K_D Fe(amp-bt) = e^{-\Delta F/2RT} = \frac{\frac{X_{Fe}^{Amp}}{1-X_{Fe}^{Amp}}}{\frac{1-X_{Fe}^{Bt}}{X_{Fe}^{Bt}}},$$

$$where\ X_{Fe} = Fe^{2+} / \sum octahederal\ sites.$$

Accordingly, if biotite and amphibole formed at the same temperature and if the Fe content was not affected by the brine fluids, then, according to this expression, plots of XFe/(1-XFe) of amphibole vs. that of biotite would give linear trends with zero

intercept at a given temperature and increasing inclination with increasing temperature (Cooper, 1972). Increased incorporation of Fe over Mg in amphibole with increasing temperature is clearly expressed in the following citation from Ramberg (1952):
"*The problem of how Al in 4-coordination affects the valency property of oxygen and thus the Mg-Fe distribution can now be considered. When the electropositive Al is placed in the site of the more electronegative Si, the bonds to the neighboring oxygen atoms become ionic and, in particular, of less double-bond character, and, as a consequence, the bonds from the neighboring non bridging oxygen toward metal ions become more covalent (see fig. 9 [here* Figure 19 *]). We can therefore conclude that, by substituting Al for Si in the silicate structure, the electronegativity of the oxygen decreases and* ***the Fe/Mg ratio is likely to increase, all other conditions being equal***."

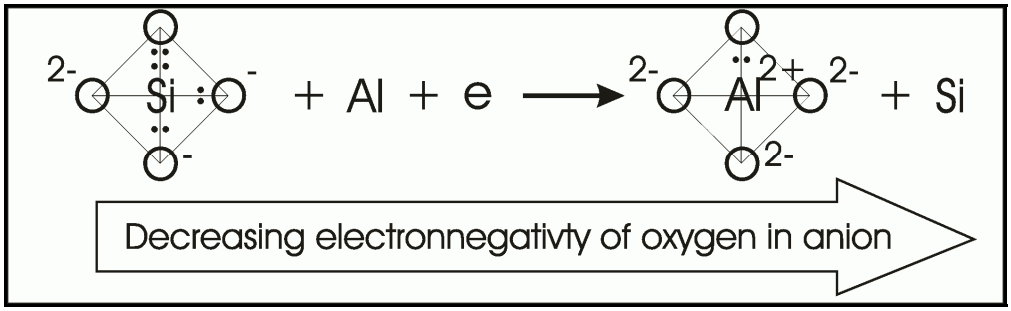

Figure 19: The change in electronegativity of oxygen in AO_4^{x-} when Si is replaced by Al. Redrawn from Ramberg (1952).

Because tetradrally coordinated Al increases in amphibole with increasing metamorphic grade then according to the above statement, the Fe/Mg ratio in amphibole will increase as an effect of the Al substitution. The increase in Al^{IV} in biotite is less than that of amphibole. As a direct consequence of this K_DFe (amp-bt) increase with temperature. (Cooper, 1972) tested this theory by plotting values of K_DFe (amp-bt) against amphibole Al^{IV} and found a general correlation although many outliers were attributed to other factors also being important. Figure 20 displays a plot of KdFe for the Froland data. There is a convincing linear correlation, which, however has a non-zero intercept. Utilizing the principle of Ramberg this is inferred as the result of different temperature at each data point. It may also be reasoned that the linear correlation reflect that amphibole and biotite were buffered by a fluid with constant salinity during cooling and exhumation and that equilibrium was achieved because of the linearity of the K_DFe(amp-bt) plot.

Given this scenario the variation between the Cl-contents of coexisting amphibole and biotite may also be interpreted. The observed complexity of the amphibole and biotite relates to the way that Cl affects the lattice and SRO (short range order in the minerals). If Fe-F and Mg-Cl avoidance was the governing factor of Cl incorporation in amphibole , one might expect LRO between Fe and Cl and that the incorporation of

Fe would change the amphibole structure in order to make space for the large Cl ion in the A site. This is not confirmed by X-ray structural refinement analysis of Cl-bearing amphiboles (Makino et al., 1993; Oberti et al., 1993). Here, it is documented that the introduction of Cl in the amphibole lattice induces local deformation of the lattice structure and increasing cell volume. The Fe enrichment in Cl-rich amphibole is due to SRO (short range order) between Fe and Cl (Oberti et al., 1993). Oberti et al (1993) also suggested that the incorporation of Cl in amphibole promotes incorporation of K in the A site and substitution of Al for Si in the tetrahedral sites. This in good agreement with the general compositional variations in amphibole (Kullerud et al., 2000, and references therein) and also the trends observed in our study. Because Cl-incorporation increase the cell volume of amphibole (Oberti et al., 1993) it is expected that the Cl incorporation depends positively on temperature. In addition Oberti et al. (1993) suggested that increased size of the octahedral sites forced an increased size of the tetrahedral sites, hence favouring Al over Si. On the contrary, if the cell volume of the mineral increases during rising T is associated with more Al^{IV} then Cl is more easily incorporated into the amphibole lattice at high than at low temperatures. Given that Al^{IV} and hence also Fe and Cl increase at a lower rate with T in biotite than in amphibole it is expected that the Cl exchange between biotite and amphibole will be temperature dependant, and at higher temperatures proportionally more Cl is incorporated in amphibole when compared to biotite. In addition the increased A site occupancy (edenite component) and K content of amphibole with increasing temperature will also promote Cl-incorporation because of the SRO between Cl and K observed by Oberti (1993). The variation in the range of edenite like substitution in biotite is less than in amphibole hence this effect is expected to be less pronounced in biotite than in amphibole. All together this agrees with our conclusions because the inferred high temperature amphiboles have higher Cl contents than co-existing biotite whereas the more evolved amphibole and biotite pairs that formed at lower T do not show this bias.

Cl-data reported in the literature of coexisting biotite and amphibole support our conclusions. In some cases the Cl-content in amphibole is higher than in coexisting biotite (e.g. Leelanandem, 1969; Leger et al., 1996; Markl et al., 1998; Zhu et al., 1994) but higher Cl content in biotite is also common (Ekstrom, 1972; Zhu et al., 1994). From the above discussion we conclude that T is the most important parameter in controlling the Cl-content. Accordingly, upper amphibolite to granulite facies amphiboles are often more Cl and Fe rich than coexisting biotite (Kullerud, 1996; Leelanandem, 1969; Leger et al., 1996; Markl et al., 1998) whereas amphiboles from lower grade contain less Cl and Fe than coexisting biotite (e.g. Ekstrom, 1972; Zhu et al., 1994). Similar to our findings, Nijland et al. (1993a) found that biotite and amphibole display varying Cl-ratios with biotite mostly being more Cl-rich than amphibole, but with the opposite being common.

Our results show that there may be many explanations of univariant Cl-element trends in amphibole and biotite. In our study the univariant trends are caused by

gradual changes in P and T in amphibolites interacting with fluids of constant salinity, whereas other studies document changes in the fluid composition at fixed PT.

It should be emphasised that not all elements composing the amphibole rims are aligned along the same univariant trends. One of the most important observations is that the trends with Mg, Fe and Cl feature several parallel but vertically offset trends. This is attributed to variations in the bulk chemical environment, i.e. the protholith.

So far the qualities of natural and experimental calibrations do not allow for the use of Cl in amphibole or biotite in a direct quantitative assessment of the fluid composition. Until better data are available, fluid inclusions by far is the most reliable tool in quantifying the fluid composition in magmatic and metamorphic environments.

One of the most important issues to keep in mind is that Cl and F-bearing fluids influence the chemistry of hydrous silicates. Accordingly, this is an important factor in ore genesis. Furthermore it may influence exchange equilibria between silicates used for thermobarometric calculations. As an example garnet biotite Fe-Mg exchange is strongly affected. Kullerud (1995) found that Cl affected the Fe-Mg exchange vector between garnet and biotite and that a correction of K_DFe-Mg (bt-grt) could be made for the biotite garnet pairs using X_{Ti}^{bt} and X_{Cl}^{bt}:

$$\ln K_D(corrected) = \ln\left[(X_{Fe}^{bt} / X_{Mg}^{bt}) / (X_{Fe}^{grt} / X_{Mg}^{grt})\right] - 2.60 X_{Ti}^{bt} - 5.67 X_{Cl}^{bt}$$

This correction, however, is probably not generally applicable to garnet-biotite thermometry because the expression lnK_DFe-Mg on X_{Ti}^{bt} and X_{Cl}^{bt} is sensitive to variations in temperature (Kullerud, 1995). Zhu and Sverjensky (1992) suggested an alternative correction for the effect of Cl in biotite on lnK_DFe-Mg based on the activity of Cl-annite which they retrieved from the experiments of Munoz and Swenson (1981). This model however underestimate the effect of Cl in the study of Kullerud (1995), probably because of the uncertainties in the Munoz and Swenson (1981) data but also because of the ideal and random mixing models used for Mg, Fe, OH and Cl used in their retrieval (Kullerud, 1995). In conclusion no thermodynamic expression may fully compensate for the effect of Cl upon the Fe-Mg exchange between biotite and other Fe-Mg silicates.

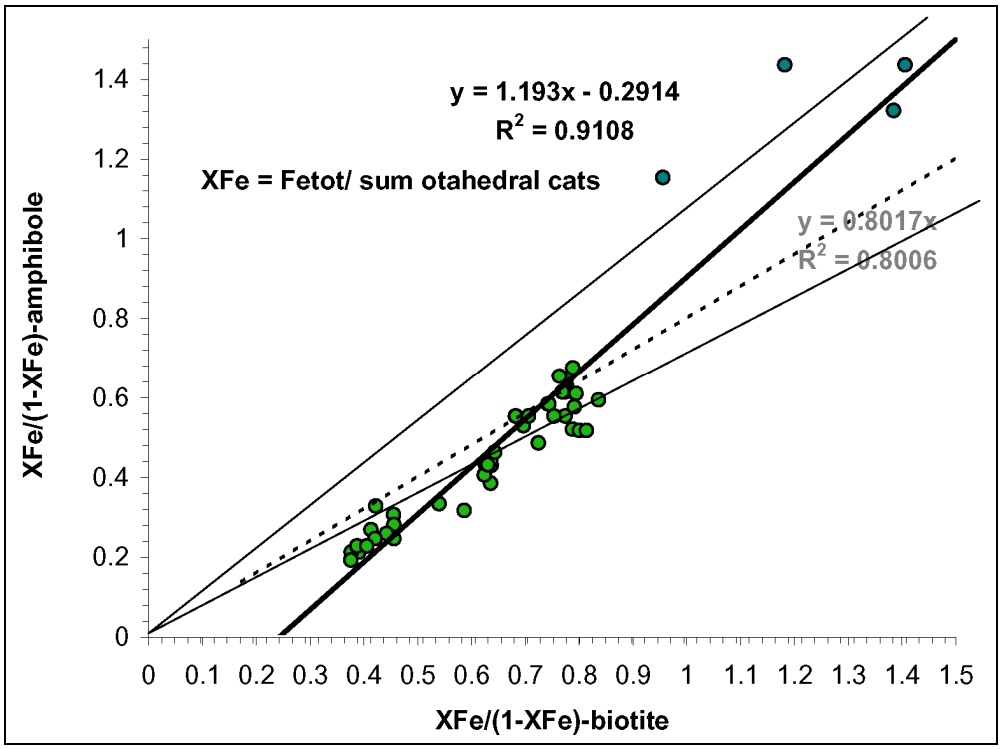

Figure 20: Comparison of KdFe of amphibole-biotite pairs. Note that there is a linear collation with a non-zero intercept. See text for discussion.

5.3 Cl-OH-F in apatite and scapolite

Whereas F was not detected in the studied amphibole and biotite, apatite features an evolution from Cl-OH apatite in the garnet quartz symplectites toward increasingly F-rich apatite parallel with the amphiboles and biotites becoming Mg-rich and Cl poor. However, most hydrothermal apatite is F-rich due to the high partitioning of F in favour of apatite. The $\log(aHCl/aH_2O)/\log(aHF/aH_2O)$ of Zhu and Sverjensky (1991) show that only small amounts of F ($\log(aF/aH_2O = 10^{-6})$ in the fluid would suffice to give F-apatite fractions of 0.9 in a 5 molal Cl- solution at 300°C. The stability field of F-apatite increase with decreasing temperature (Zhu and Sverjensky, 1991) hence F-enrichment in the Froland-apatite probably reflect dropping temperature and not F-enrichment in the fluid.

Y and Ce are relatively enriched in early apatites in garnet-quartz symplectites whereas intermediate OH-F apatite coexisting with amp3 is low in both Y and Ce. Late F-apatite coexisting with amp4 is relatively enriched in Y. Harlov and co-workers (2003; 2002) studied the alteration of Cl-apatite from Ødegårdens Verk, Bamble Sector and replicated observed chemical evolution by hydrothermal alteration experiments.

Their results imply that, mostly, the alteration of Cl-apatite is a function of fluid composition and that P and T are less significant. Hydrothermal alteration with H_2O-rich fluids is more effective in removing Y+REE from Cl-apatite than F-rich aqueous fluids, probably because F^- stabilise Y in the apatite lattice (Harlov et al., 2002). The depletion of Ce andY in the intermediate apatite in our study agrees with the depletion observed by Harlov and co-workers (2002) by alteration with a H_2O-rich fluid. In agreement with the observation by Harlov and co-workers (2002) the enrichment of Y in late F-rich apatite is a product of the F-enrichment.

We only studied a limited number of apatite samples in our study and focussed mainly on the retrograde evolution of apatite. Nijland and co-workers (1993a) studied halogen zonation patterns in apatite from amphibolite samples scattered across the Bamble Sector, which they related to the prograde fluid evolution. They conclude that systematic spatial variations across the metamorphic zones of the Bamble Sector are absent. They observe three main types of F-zonation patterns; (1) W-shaped, (2) Rimward increasing and (3) Rimward decreasing. Nijland and co-workers infer that the patterns reflect the fluid environment, with most features belonging to the prograde evolution. However, Nijland et al. (1993a) do suggest that the rimward increasing F-content (3) could have formed during either prograde or retrograde conditions due to increasing F-content in the fluid. However the rimward F-increase reported by Nijland et al. (1993a) is more likely to be due to cooling because F-apatite is stable even with a low F fluid at low temperatures (Zhu and Sverjensky, 1991). The variable patterns observed in apatite probably tell the same story as our amphibole cores that also show variable trends. Probably, this is an effect of local buffering during peak PT conditions.

From our textural observations, we infer that scapolite was late in the mineral assemblage. Although scapolite coexisted with CO_2-free fluids, scapolite formula recalculation implies that scapolite probably contained significant CO_3 and HCO_3. Accordingly, CO_2 did not come from the fluid. Textural observations imply that scapolitisation depended on the presence of both calcite and plagioclase. Similar observations were made by Visser and co-workers (1999). Therefore, we suggest that scapolite formed by a reaction involving calcite as also suggested by Visser et al. (1999):

cc + brine+ pl = scp

The strongly variable composition is mostly a function of local chemical variations, particularly in the amount of calcite, the composition of the replaced plagioclases and the Ca/Na ratio of the coexisting fluid. Given that the fluids maintained constant compositions (paper 2, Sørensen and Larsen, 2007b) it was primarily the local rock composition governed by plagioclase and calcite that buffered the scapolite composition.

5.4 Genetic interpretation of the textural evolution

The principles derived from the mineral chemistries of biotite and amphibole, respectively, provide a model that in combination with our fluid inclusion observations, may be used to understand the complex alteration textures observed on field as well as thin section scale. The amphibole trends confirm the interaction with brines of more ore less constant salinity during cooling and exhumation.

The first alteration type are potassic and occur as the introduction of Fe-rich biotite and amphibole overgrowths comprising the blue green ferrotschermakites observed at locality 1 (Amp3a). The Al^{IV} and Fe content of these rims are higher than in the amphibole cores. However, as the temperature decreased the amphibole rims became more Mg-rich and Al poor than the cores, comprising magnesiohornblende. Early alteration assemblages contain calcite, suggesting that the fluid contained CO_2. This is confirmed by the FIA2 fluid inclusions (see Sørensen and Larsen (paper2, Sørensen and Larsen, 2007b).

Elements were redistributed on both hand specimen and field scale in the amphibolites. The most prominent example of this process is the conspicuous modal differentiation characterising the amphibolite in generating areas dominated by biotite and amphibole, biotite and plagioclase, biotite and plagioclase etc. The zoning observed at the plagioclase veins at locality 5 and the border zones around the en echelon veins at locality 4 are good examples of this effect. This principle is most easily illustrated by the mineralogical zonation in the alteration zones associated with the plagioclase veins at locality 5:

The central zone1 is enriched in ilmenite, Ca CO_2 Fe and sulphur; this is followed by a zone free of biotite mainly comprising plagioclase and amphibole, followed by an amphibole free zone mainly comprising biotite and plagioclase. This local scale observation may possibly mirror the metasomatic processes at a much larger scale throughout the Bamble Sector. I.e. Fe and other elements are removed from the amphibolites and redeposited elsewhere giving rise to the numerous Fe-deposits as well as Fe-Cu oxide/sulphide deposits across the Bamble sector. This is also suggested by Brøgger (1934) for the breccia related deposits at Langøy that formed when mafic rocks were altered by scapolitisation and albitisation processes. Korneliussen et al.(2000) suggest this as a general genetic model for the Fe-Cu deposits in the Bamble Sector.

Genetic models of ore deposits would benefit from an increased understanding of the interaction of fluids with silicates in the wall rocks because fluid-rock interactions in the wall rock probably explain many element enrichments leading to ore formation. Bearing this in mind, we find it peculiar that many studies of ore deposits use the (Munoz, 1992; Munoz and Swenson, 1981) models to calculate halogen activities in ore forming fluids because the model assumes that crystal chemical constraint are in control of the halogen contents of biotite and amphibole. Rather we suggest that the fluid phase pose a partial control on the mineral chemistry and that fluid rock interaction leads to changes in mineral and fluid composition in order to obtain

equilibrium conditions. As parameters such as pressure, temperature, fluid composition and fluid-rock ratios changes the equilibria also changes.

In our study the mineralogical changes are provoked by fluid rock interaction with a fluid of constant salinity during cooling and exhumation.

However, the understanding of the architecture and tectono-metamorphic evolution of the Bamble Sector remain fragmentary. Partially because the importance of massive pulses of highly saline fluids were not fully appreciated. Our study concerns a rather limited portion of the Bamble Sector, however, it is one of the few studies that documents the importance of highly saline aqueous fluids and demonstrates the implications for the mineralogy and metasomatic processes on micro as well as macro scale. Studies by Cameron (1993a; 1993b) and Cameron and co-workers (1993) document the mobilisation of Au and other chalcophile elements during high grade metamorphism and retrogression in the Bamble Sector through analysis of the whole rock chemistry. Their results document how chalcophile elements are depleted through amphibolitisation of coronitic gabbro at high f_{O2} (Cameron et al., 1993) and reintroduced in retrograde veins focussed at higher crustal levels near the brittle-ductile transition (Cameron, 1993b).

Ti-phases experience a gradual evolution as exemplified by cores of rutile that are overgrown/replaced by rims of ilmenite which again are overgrown/replaced by titanite. The replacement of rutile by ilmenite is easily explained by the gradual loss of Fe from the Fe-Mg silicates biotite and amphibole.

On the contrary, the replacement of ilmenite by titanite is more difficult to explain. Harlov et al. (2006) suggests that the titanite rims formed due to the reactions:

$$\text{cpx} + \text{ilm} + \text{quartz} + H_2O = \text{amphibole} + \text{titanite (hydration)}$$

or

$$\text{amphibole} + \text{ilmenite} + O_2 = \text{titanite} + \text{magnetite} + \text{quartz} + H_2O$$

The general absence of clinopyroxene and magnetite in our samples, however, precludes the above reactions. Rather, it is inferred that metasomatism is involved. Calcite is commonly observed in vicinity of the replacement rims hence may be the source of Ca in titanite together with plagioclase that also becomes more albite rich as metasomatic alteration proceeds. The Fe lost by the ilmenite is likely to have formed sulphides as petrographic observations suggest that pyrite in some cases formed together with the titanite rims.

Potassic alteration with biotite was followed by potassic alteration where biotite was replaced by K-feldspar. No Fe/Mg phase seem to increase during this stage hence suggesting that the replacement involved mobilisation of Mg as well as Fe. In relation to this replacement, ilmenite is all most completely replaced with titanite, suggesting that the replacement of ilmenite by titanite belongs to the same metasomatic event.

Scapolitisation involves the replacement of plagioclase + calcite by scapolite and ilmenite and rutile by titanite.

5.5 The metamorphic evolution of the area as experienced by amphibolites

Based on this discussion we summarise the metamorphic evolution as experienced by the amphibolites as follows:

1. Amphibolitisation of gabbro: Field and petrographic evidence document the gradual amphibolitisation of gabbro. This relates to the formation of garnet bearing amphibolites. Notably the chemistry of amphiboles in the garnet bearing amphibolites is dissociated from the evolution in non-garnet bearing amphibolites. This is especially clear when it comes to Cl and Fe.
2. Oxidation of garnet amphibolite. The amphiboles in the garnet amphibolites show high estimated Fe^{3+}. This may reflect oxidation because charge compensation is not completely obtained by the measured elements.
3. Formation of partial melts (the garnet quartz symplectites).
4. Formation of garnet free amphibolites
5. Retrogression and metasomatism of amphibolite during exhumation.
    a. Introduction of K-bearing CO_2-H_2O solutions and formation of biotite, amphibole overgrowth rims and en echelon quartz veins, gradual loss of CO_2 from the fluid phase
    b. Formation of K-feldspar at the expense of biotite and plagioclase. Change in fluid composition due to loss of K in the fluid-rock interaction related to mineral reactions.
    c. Scapolitisation, characterised by replacement of plagioclase by scapolite (EqAn = 41.3-59.5). Apparently this reaction correlates with CO_2 free fluid inclusions in nearby quartz.

Our results underline the importance of highly saline aqueous fluids in the retrogression of amphibolites. Unaltered high-grade amphibolite is juxtaposed with completely altered and chemically transformed rock that once was amphibolite. The most prominent chemical alteration experienced by the amphibolites is the enrichment in potassium, marked by the introduction of biotite and K-feldspar.

In addition our results confirm the ore formation models suggested by (Brøgger, 1934; Korneliussen et al., 2000) in which the ore deposits situated proximally and distally to the altered amphibolites are the ultimate results of the depletion processes in the amphibolites. Mass transfer was controlled by equilibria between brines of almost constant salinity and mineral assemblages during cooling and uplift.

6 References

Ahall, K.I. and Gower, C.F., 1997. The Gothian and Labradorian orogens; variations in accretionary tectonism along a late Paleoproterozoic Laurentia-Baltica margin. GFF, 119(2): 181-191.

Austrheim, H., 2006. Potassic alteration in association with scapolitisation of metagabbro at Langøy, eastern Bamble (personal communication to Bjørn Eske Sørensen by telephone 13 december 2006). Discussion the occurrence of potassic alteration in eastern Bamble. Håkon Austrheim had noted that in relation with alteration of metagabbro biotite was introduced as a new mineral, commonly together with scapolite and prehnite. The most intensely scapolitilsed zones are rich in coarse grained Cl-rich biotite, which does not belong to the original metagabbro mineralogy. This suggest that potassium was introduced during the alteration since the protolith had low potassium content. The observations reported by Håkon Austrheim are preliminary observations in a study together with Ane K. Engvik about the scapolitisation process at Langøy.

Bingen, B., Boven, A., Punzalan, L., Wijbrans, J.R. and Demaiffe, D., 1998. Hornblende (super 40) Ar/ (super 39) Ar geochronology across terrane boundaries in the Sveconorwegian Province of S. Norway. Precambrian Research, 90: 159-185.

Bingen, B., Mansfeld, J., Sigmond, E.M.O. and Stein, H., 2002. Baltica-Laurentia link during the Mesoproterozoic; 1.27 Ga development of continental basins in the Sveconorwegian Orogen, southern Norway. Canadian Journal of Earth Sciences = Revue Canadienne des Sciences de la Terre, 39(9): 1425-1440.

Bingen, B., Nordgulen, Ø. and Sigmond, E.M.O., 2001. Correlation of supracrustal sequences and origin of terranes in the Sweconorwegian orogen of SW Scandinavia: SIMS data on zircon in clastic metasediments. Precambran Research 108: 293-318.

Bingen, B. and Van-Breemen, O., 1998. Tectonic regimes and terrane boundaries in the high-grade Sveconorwegian Belt of SW Norway, inferred from U-Pb zircon geochronology and geochemical signature of augen gneiss suites. J. Geol. Soc. Lond. , 155: 143-154.

Brickwood, J.D. and Craig, J.W., 1987. Primary and reequilibrated mineral assemblages from the Kongsdberg and Bamble areas, Norway. Norges Geologiske Undersøkelse, 410: 1-23.

Brøgger, W.C., 1934. On several Archean rocks from the south coast of Norway; II, The south Norwegian hyperites and their metamorphism. 1; 1, 421 pp.

Bugge, A., 1965. Iakttagelser fra rektangelbladet Kragerø og den store grunnfjellsbreksje. Norges Geologiske Undersøkelse, 229: 115p.

Bugge, J.A.W., 1940. Geological and petrological investigations of the Arendal district. Norsk Geologisk Tidsskrift, 20: 71-112.

Cameron, E.M., 1993a. Precambrian gold - perspectives from the top and bottom of shear zones. Canadian Mineralogist, 31: 917-944.

Cameron, E.M., 1993b. Reintroduction of gold, other chalcophile elements and LILE during retrogression of depleted granulite, Tromoy, Norway. Lithos, 29(3-4): 303-309.

Cameron, E.M., Cogulu, E.H. and Stirling, J., 1993. Mobilization of gold in the deep crust - Evidence from mafic intrusions in the Bamble Belt, Norway. Lithos, 30(2): 151-166.

Clowe, C.A., Popp, R.K. and Fritz, S.J., 1988. Experimental investigation of the effect of oxygen fugacity on ferric-ferrous ratios and unit-cell parameters of 4 natural clinoamphiboles. American Mineralogist, 73(5-6): 487-499.

Cooper, A.F., 1972. Progressive metamorphism of metabasic rocks from Haast Schist Group of Southern New Zealand. Journal of Petrology, 13(3): 457-492.

Cosca, M.A., Essene, E.J. and Bowman, J.R., 1991. Complete chemical-analyses of metamorphic hornblendes - Implications for normalizations, calculated H_2O Activities, and thermobarometry. Contributions to Mineralogy and Petrology, 108(4): 472-484.

Cosca, M.A., Mezger, K. and Essene, E.J., 1998. The Baltica-Laurentia connection Sveconorwegian (Grenvillian) metamorphism, cooling, and unroofing in the Bamble sector, Norway. Journal of Geology, 106: 539-552.

Dahlgren, S., Bogoch, R., Magaritz, M. and Michard, A., 1993. Hydrothermal dolomite marbles associated with charnockitic magmatism in the Proterozoic Bamble Shear Belt, South Norway. Contributions to Mineralogy and Petrology, 113(3): 394-409.

Ekstrom, T.K., 1972. Coexisting scapolite and plagioclase from two iron formations in northern Sweden. Lithos, 5: 175-185.

Elliott, R.B., 1966. Association of amphibolite and albitite, Kragero South Norway. Geological Magazine, 103(1): 1-7.

Falkum, T. and Petersen, J.S., 1980. The Sveconorwegian orogenic belt, a case of late-Proterozoic plate-collision. Geologische Rundshcau, 69: 622-647.

Field, D., Drury, S. and Cooper, D.C., 1980. Rare-earth and LIL element fractionation in high-grade charnockitic gneisses, South Norway. Lithos 13: 281-289.

Frodesen, S., 1968. Petrographical and chemical investigations of a precambrian gabbro intrusion, Hiåsen, Bamble area, south Norway. Norsk Geologisk Tidsskrift, 48: 281-306.

Gualda, G.A.R. and Vlach, S.R.F., 2005. Stoichiometry-based estimates of ferric iron in calcic, sodic-calcic and sodic amphiboles: A comparison of various methods. Anais Da Academia Brasileira De Ciencias, 77(3): 521-534.

Harlov, D., Tropper, P., Seifert, W., Nijland, T. and Forster, H.J., 2006. Formation of Al-rich titanite ($CaTiSiO_4O$-$CaAlSiO_4OH$) reaction rims on ilmenite in metamorphic rocks as a function of fH_2O and fO_2. Lithos, 88(1-4): 72-84.

Harlov, D.E., 1992. Comparative oxygen barometry in granulites, Bamble sector, SE Norway. Journal of Geology, 100: 447-464

Harlov, D.E., 2000a. Pressure-temperature estimation in orthopyroxene-garnet bearing granulite facies rocks, Bamble sector, Norway. Mineralogy and Petrology, 69: 11-33.

Harlov, D.E., 2000b. Titaniferous magnetite-ilmenite thermometry and titaniferous magnetite-ilmenite-orthopyroxene-quartz oxygen barometry in granulite facies gneisses, Bamble sector, SE Norway; implications for the role of high-grade CO_2-rich fluids during granulite genesis. Contributions to Mineralogy and Petrology 139: 180-197

Harlov, D.E. and Foerster, H.J., 2003. Fluid-induced nucleation of (Y+REE)-phosphate minerals within apatite; nature and experiment; Part II, Fluorapatite. American Mineralogist, 88(8-9): 1209-1229.

Harlov, D.E., Foerster, H.J. and Nijland, T.G., 2002. Fluid-induced nucleation of (Y + REE)-phosphate minerals within apatite; nature and experiment; Part I, Chlorapatite. American Mineralogist, 87(2-3): 245-261.

Henderson, I.H.C. and Ihlen, P.M., 2004. Emplacement of polygeneration pegmatites in relation to Sveco-Norwegian contractional tectonics; examples from southern Norway. Precambrian Research, 133(3-4): 207-222.

Johansson, L. and Kullerud, L., 1993. Late Sveconorwegian metamorphism and defromation in southwestern Sweden. Precambrain Research, 64: 347-360.

Jøsang, O., 1966. Geologiske og petrografiske undersøkelser i Modumfeltet. Norges Geologiske Undersøkelse, 235: 148p.

Knudsen, T.L., 1996. Petrology and geothermobarometry of granulite facies metapelites from the Hisøy-Torungen area, South Norway; new data on the Sveconorvegian P-T-t path of the Bamble sector. Journal of Metamorphic Geology, 14(3): 267-287.

Knudsen, T.L. and Andersen, T., 1999. Petrology and geochemistry of the Tromøy gneiss complex, South Norway; an alleged example of Proterozoic depleted lower continental crust. Journal of Petrology 40: 909-933.

Knudsen, T.L., Andersen, T., Maijer, C. and Verschure, R.H., 1997. Trace-element characteristics and Pb isotopic evolution of metasediments and associated Proterozoic rocks from the amphibolite- to granulite-facies Bamble sector, Southern Norway. Chemical Geology, 143(3-4): 145-169.

Knudsen, T.L. and Lidwin, A., 1996. Magmatic CO_2, brine and nitrogen inclusions in Sveconorwegian enderbitic dehydration veins and a gabbro from the Bamble sector, southern Norway. European Journal of Mineralogy, 8: 1041-1063.

Konnerup-Madsen, J., 1979. Fluid Inclusions in Quartz from Deep-Seated Granitic Intrusions, South-Norway. Lithos, 12(1): 13-23.

Korneliussen, A., Dahlgren, S., Ihlen, P.M. and Sandstad, J.S., 2000. On the relationships between metasomatic processes (scapolitisation) at deep crustal levels and fracture-bound ore deposits in the Bamble sector of the Fennoscandian Shield, S. Norway. In: P. Weihed and O. Martinsson (Editors), 2nd annual GEODE-Fennoscandian shield workshop on Paleoproterozoic and Archean greenstone belts and VMS districts in the Fennoscandian Shield Luleå University of Technology Research Report Gällivare-Kiruna, Sweden, pp. 22-25.

Kullerud, K., 1995. Chlorine, titanium and barium-rich biotites - Factors controlling biotite composition and the Implications for garnet-biotite geothermometry. Contributions to Mineralogy and Petrology, 120(1): 42-59.

Kullerud, K., 1996. Chlorine-rich amphiboles: Interplay between amphibole composition and an evolving fluid. European Journal of Mineralogy, 8(2): 355-370.

Kullerud, K. and Erambert, M., 1999. Cl-scapolite, Cl-amphibole, and plagioclase equilibria in ductile shear zones at Nusfjord, Lofoten, Norway: Implications for fluid compositional evolution during fluid-mineral interaction in the deep crust. Geochimica et Cosmochimica Acta, 63: 3829-3844.

Kullerud, K., Flaat, K. and Davidsen, B., 2000. Occurrence and origin of Cl-rich amphibole and biotite in the Earth's crust - implications for fluid composition and evolution. In: I. Stober and K. Bucher (Editors), Hydrogeology of crystalline rocks. Kluwer Academic Publishers, Netherlands, pp. 205-225.

Kullerud, K. and Machado, N., 1991. End of a controversy; U-Pb geochronological geochronological evidence for significant Grenvillian activity in the Bamble area, Norway., Sixth Meeting of the European Union of Geosciences. Terra Abstracts, pp. 504.

Kullerud, L. and Dahlgren, S., 1993. Sm-Nd geochronology of Sveconorwegian granulite facies mineral assemblages in the Bamble shear belt, South Norway. Precambrian Ressearch 64: 389-402.

Lamb, R.C., Smalley, P.C. and Field, D., 1986. P-T conditions for the Arendal granulites, southern Norway; implications for the roles of P, T and CO_2 in deep crustal LILE-depletion. Journal of Metamorphic Geology 4: 143-160.

Leelanandem, C., 1969. Electron microprobe analyses of chlorine in hornblendes and biotites from charnockitic rocks of Kondapall, India. Mineralogical Magazine, 37(287): 362-365.

Leger, A., Rebbert, C. and Webster, J., 1996. Cl-rich biotite and amphibole from Black Rock Forest, Cornwall, New York. American Mineralogist, 81(3-4): 495-504.

Lieftink, D.J., Nijland, T.G. and Maijer, C., 1993. Cl-rich scapolite from Ødegardens Verk, Bamble, Norway. Norsk Geologisk Tidsskrift, 73(1): 55-57.

Lieftink, D.J., Nijland, T.G. and Maijer, C., 1994. The behavior of rare-earth elements in high-temperature Cl-bearing aqueous fluids; results from the Ødegardens Verk natural laboratory. The Canadian Mineralogist, 32 Part 1: 149-158.

Makino, K., Tomita, K. and Suwa, K., 1993. Effect of chlorine on the crystal-structure of a chlorine-rich hastingsite. Mineralogical Magazine, 57(389): 677-685.

Markl, G., Ferry, J. and Bucher, K., 1998. Formation of saline brines and salt in the lower crust by hydration reactions in partially retrogressed granulites

from the Lofoten Islands, Norway. American Journal of Science, 298(9): 705-757.
Morton, R.D., Batey, R. and O'Nions, R.K., 1970. Geological investigations in the Bamble sector of the Fennoscandian Shield south Norway. 1. The geology of eastern Bamble. Norges Geologiske Undersøkelse, 263, 61 pp.
Munoz, J.L., 1992. Calculation of HF and HCl fugacites from biotite compositions; revised equations. Geological Society of America Abstracts with Programs, 24: 221.
Munoz, J.L. and Swenson, A., 1981. Chloride-hydroxyl exchange in biotite and estimation of relative HCl/HF activities in hydrothermal fluids. Economic Geology, 76(8): 2212-2221.
Munz, I.A., Wayne, D. and Austrheim, H., 1994. Retrograde fluid infiltration in the high-grade Modum Complex, South Norway - Evidence for age, source and REE mobility. Contributions to Mineralogy and Petrology, 116(1-2): 32-46.
Munz, I.A., Yardley, B.W.D., Banks, D.A. and Wayne, D., 1995. Deep penetration of sedimentary fluids in basement rocks from Southern Norway - Evidence from hydrocarbon and brine inclusions in quartz veins. Geochimica Et Cosmochimica Acta, 59(2): 239-254.
Nijland, T.G., 1989. De Geologie van het Nelaug gebeid, Bamble sector, Zuid Noorwegen. Unpublished Masters Degree Thesis, Utrecht university, Utrecht, 85 pp.
Nijland, T.G., Jansen, J.B.H. and Maijer, C., 1993a. Halogen geochemistry of fluid during amphibolite-granulite metamorphism as indicated by apatite and hydrous silicates in basic rocks from the Bamble sector, South Norway. Lithos, 30(2): 167-189.
Nijland, T.G., Liauw, F., Visser, D., Maijer, C. and Senior, A., 1993b. Metamorphic petrology of the Froland corundum-bearing rocks; the cooling and uplift history of the Bamble sector, South Norway. Bulletin - Norges Geologiske Undersokelse, 424: 51-63.
Nijland, T.G. and Maijer, C., 1993. The regional amphibolite to granulite facies transition at Arendal, Norway; evidence for a thermal dome. Neues Jahrbuch fuer Mineralogie Abhandlungen, 165: 191-221.
Nijland, T.G. and Touret, J.L.R., 2001. Replacement of graphic pegmatite by graphic albite-actinolite-clinopyroxene intergrowths (Mjavatn, southern Norway). European Journal of Mineralogy, 13(1): 41-50.
Nijland, T.G., Touret, J.L.R. and Visser, D., 1998. Anomalously low temperature orthopyroxene, spinel, and sapphirine occurrences in

metasediments from the Bamble amphibolite-to-granulite facies transition zone (South Norway); possible evidence for localized action of saline fluids. Journal of Geology, 106(5): 575-590.

Nijland, T.G. and Visser, D., 1995. The Provenance of Bamble Amphibolites, Norway. Proceedings of the Koninklijke Nederlandse Akademie Van Wetenschappen-Biological Chemical Geological Physical and Medical Sciences, 98(1): 69-88.

Oberti, R., Ungaretti, L., Cannillo, E. and Hawthorne, F.C., 1993. The mechanism of Cl Incorporation in amphibole. American Mineralogist, 78(7-8): 746-752.

Popp, R.K., Virgo, D. and Phillips, M.W., 1995. H deficiency in kaersutitic amphiboles: Experimental verification. American Mineralogist, 80(11-12): 1347-1350.

Ramberg, H., 1952. Chemical bonds and distribution of cations in silicates. Journal of Geology, 60(4): 331-355.

Sato, H., Holtz, F., Behrens, H., Botcharnikov, R. and Nakada, S., 2005. Experimental petrology of the 1991-1995 Unzen dacite, Japan. Part II: Cl/OH partitioning between hornblende and melt and its implications for the origin of oscillatory zoning of hornblende phenocrysts. Journal of Petrology, 46(2): 339-354.

Smalley, P.C., Field, D., Lamb, R.C. and Clough, P.W.L., 1983. Rare earth, Th-Hf-Ta and large-ion lithophile element variations in metabasites from the Proterozoic amphibolite-granulite transition zone at Arendal, South Norway. Earth Planet Scientiffic Letters, 63: 446-458.

Sørensen, B.E. and Larsen, R.B., 2007a. Paper1: Fluid induced multistage recrystallisation microstructures in quartzites and quartz veins from the Bamble shear zone complex. In: B.E. Sørensen (Editor), Metamorphic refinement of quartz under influence of fluids during exhumation with reference to the metamorphic/metasomatic evolution observed in amphibolites - a detailed field, microtectonic and geochemical study from the Bamble sector, South Norway. PhD Thesis, Department of Geology and Mineral Resources Engineering, NTNU Trondheim.

Sørensen, B.E. and Larsen, R.B., 2007b. Paper2: The fluid evolution of the Froland area in the Bamble sector from peak P-T through cooling and uplift: implications for retrograde mineral paragenesis and PT evolution of the Bamble sector. In: B.E. Sørensen (Editor), Metamorphic refinement of quartz under influence of fluids during exhumation with reference to the metamorphic/metasomatic evolution observed in amphibolites - a detailed field, microtectonic and geochemical study

from the Bamble sector, South Norway. PhD Thesis, Department of Geology and Mineral Resources Engineering, NTNU Trondheim.
Starmer, I.C., 1985. The evolution of the South Norwegian Proterozoic as revealed by major and mega-tectonics of the Kongsberg and Bamble sectors. In: J.L.R. Touret and A.C. Tobi (Editors), The deep Proterozoic crust of the North Atlantic Provinces. Reidel, Dordrecht, pp. 259-290.
Starmer, I.C., 1987. The geological map of the Bamble sector, South Norway, The geology of southernmost Norway: A geological excursion guide with thematic articles prepared for the NATO advanced study institute. Special Publication Geological Survey of Norway, pp. 25.
Starmer, I.C., 1991. The proterozoic evolution of the Bamble sector, Southern Norway; correlation across southern Scandinavia and the Grenvillian controversy. Precambrain Research, 49: 107-139.
Starmer, I.C., 1993. The Sweconorwegian Orogeny in Southern Norway, relative to deep crustal structures and events in the North Atlantic Proterozoic supercontinent. Norsk Geologisk Tidsskrift, 73: 109-132.
Starmer, I.C., 1996. Accretion, rifting, rotation and collision in the North Atlantic supercontinent, 1700-950 Ma. In: Precambrain crustal evolution in the North Atlantic Region. Geological Society of London Special Publications, 112: 219-248.
Teertstra, D.K. and Sheriff, B.L., 1997. Substitutional mechanisms, compositional trends and end member formulae of scapolite. Chemical Geology, 136: 233-260.
Touret, J., 1968. The Precambrian metamorphic rocks around the Lake Vegår (Aust-Agder, southern Norway). Norges Geologiske Undersøkelse, 257, 45 pp.
Touret, J., 1971. Le faciès granulite en Norvège méridionale II Les inclusions fluides. Lithos, 4: 423-436.
Touret, J., 1972. Le faciès granulite en Norvège méridionale et Les inclusions fluides. . Sci. Terre 17: 179-193.
Touret, J., 1985. Fluid regime in southern Norway: the record of fluid inclusions. In: A.C. Tobi and J. Touret (Editors), The deep Proterozoic crust in the North Atlantic Provinces NATO ASI Ser. Ser. C: Math. Phys. Sci., pp. 517-549.
Touret, J. and Olsen, S.N., 1985. Fluid inclusions in migmatites. In: J.R. Ashworth (Editor), Migmatites. Shiva, Glasgow, pp. 265-288.
Van den Kerkhof, A.M., Kreulen, R. and Touret, J.L.R., 1994. Juvenile CO_2 in enderbites of Tromøy near Arendal, southern Norway: a fluid inclusion and stable isotope study. Journal of Metamorphic Geology, 12: 301-310.

Visser, D., Nijland, T.G., Lieftink, D.J. and Maijer, C., 1999. The occurrence of preiswerkite in a tourmaline-biotite-scapolite rock from Blengsvatn, Norway. American Mineralogist, 84(5-6): 977-982.

Xiao, Y.L., Hoefs, J. and Kronz, A., 2005. Compositionally zoned Cl-rich amphiboles from North Dabie Shan, China: Monitor of high-pressure metamorphic fluid/rock interaction processes. Lithos, 81(1-4): 279-295.

Zhu, C. et al., 1994. Tem-Aem observations of Cl-rich amphibole and biotite and possible petrologic implications. American Mineralogist, 79(9-10): 909-920.

Zhu, C. and Sverjensky, D.A., 1991. Partitioning of F-Cl-OH between minerals and hydrothermal fluids. Geochimica Et Cosmochimica Acta, 55(7): 1837-1858.

Zhu, C. and Sverjensky, D.A., 1992. F-Cl-OH Partitioning between biotite and apatite. Geochimica Et Cosmochimica Acta, 56(9): 3435-3467.